

General Disclaimer

One or more of the Following Statements may affect this Document

- This document has been reproduced from the best copy furnished by the organizational source. It is being released in the interest of making available as much information as possible.
- This document may contain data, which exceeds the sheet parameters. It was furnished in this condition by the organizational source and is the best copy available.
- This document may contain tone-on-tone or color graphs, charts and/or pictures, which have been reproduced in black and white.
- This document is paginated as submitted by the original source.
- Portions of this document are not fully legible due to the historical nature of some of the material. However, it is the best reproduction available from the original submission.

(NASA-CR-136748) ANALYSIS OF
SELF-OSCILLATING dc-TO-dc CONVERTERS Final
Report, Feb. 1973 - Aug. 1974 (Lowell
Technological Inst. Research Foundation)
82 p HC \$4.75

N75-19542

Unclas
17272

CSCI 09E G3/33

FINAL REPORT

NGR-22-018-066

August, 1974



LOWELL TECHNOLOGICAL INSTITUTE
Lowell, Massachusetts

DEPARTMENT OF ELECTRICAL ENGINEERING

Final Report
For the period February , 1973 to
August , 1974

NASA Grant NGR-22-018-066 , entitled :

ANALYSIS OF SELF-OSCILLATING DC-TO-DC CONVERTERS

Prepared for :
NATIONAL AERONAUTICS AND SPACE ADMINISTRATION
Washington, D. C.

Prepared by :
Peter Burger
Principal Investigator

August 31 , 1974

FORWORD

In this report the principal results of one year of research are described. The research was supported by NASA Grant NGR-22-018-066 and was conducted in the Electrical Engineering Department of Lowell Technological Institute, Lowell, Mass. This report is in two parts. The first part consists of a complete paper that is being submitted for publication to the Transactions of Industrial Electronics of the IEEE. The second part consists of three appendices, which contain the detailed final results of this first year of work under this NASA Grant.

The author would like to thank his colleagues , in particular , Prof. Ronald Brunelle for his help in the analog simulation work , and Robert Dirkman , for his suggestions that were very helpful in the development of the analog simulation model. Many thanks are also due to Vincent Lalli of the Lewis Research Center of NASA , Cleveland, Ohio, for his many helpful suggestions throughout this research period. Mr. Lalli's continued encouragement is also greatly appreciated.

PART I.

Paper prepared for publication
In the IEEE Transactions of Industrial Electronics.

ANALYSIS OF A CLASS OF PULSE MODULATED DC-TO -DC POWER CONVERTERS

ABSTRACT

The basic operational characteristics of Dc-to-Dc converters are analyzed. The basic physical characteristics of power converters are indentified. A simple class of Dc-to-Dc power converters are chosen which could satisfy any set of operating requirements. Three different controlling methods in this class are described in detail. Necessary conditions for the stability of these converters are measured through analog computer simulation. These curves are related to other operational characteristics, such as ripple and regulation. Finally, further research is suggested for the solution of absolute stability and efficient physical design of this class of power converters.

ANALYSIS OF A CLASS OF
PULSE MODULATED DC-TO-DC POWER CONVERTERS *

by Peter Burger
Lowell Technological Institute
Department of Electrical Engineering
Lowell , Mass.

August , 1974

*: This Research has been supported by NASA Grant NGR-22-018-066

I. INTRODUCTION

Efficient Dc-to-Dc power conversion has been an important problem in many areas of industrial power conditioning and has been especially vital for the aerospace industry. Successful Dc-to-Dc power conversion might even become the cornerstone of dc power distribution systems of the future. Therefore, the design of reliable and efficient Dc-to-Dc power converters should demand the attention of engineers. The problem of designing reliable and efficient power converters has as yet no standard method of solution. There is no agreement between design engineers even whether such standard method could be found. We are far from claiming that we have found such a general method of design, but , we shall propose one possible approach to the design problem and through it the reader will hopefully obtain some insight into the complexity of the problem.

Before discussing the specific problems of converter design, let us review the most important factors that influence the Dc-to-Dc conversion process. Dc-to-Dc power conversion can be stated simply as the process by which power available at one dc voltage level is to be transformed to power at a different dc voltage level. It is well known that this conversion problem cannot be solved without first converting the Dc source power into a time-varying, or Ac power which then transformed and finally passed through a low pass filter for the required dc voltage level at the output. The conversion of Dc to Ac power and filtering cannot be realized without power loss, therefore the efficiency of the conversion process ($\text{efficiency} = \text{power out} / \text{power in}$) becomes an important factor.

It is also impossible to make the output filtering process perfect, therefore the output power will contain some Ac component, and the output ripple also becomes an important factor in the conversion process ($\text{ripple} = \text{output Ac component voltage magnitude} / \text{output Dc voltage level}$).

Efficiency and ripple are present even in the simplest Dc-to-Dc conversion problem when the source power and the output power are at constant levels and the load or required power is also a constant. However, real power sources have variable voltage levels. This level can be the function of required power, as in batteries, or time, as in solar sources, or both. Under such variable input voltage levels and variable loads it is not possible to keep the output Dc voltage level constant, therefore regulation becomes the next important factor (regulation = variation in output Dc voltage level/output Dc voltage level) in the conversion process.

Finally, there are transient considerations. The output load could develop a sudden short or open circuit. When the fault is removed it is of primary concern how fast the output recovers. The factor that indicates the recovery time of the converter is settling time (or time constant) which expresses the maximum time needed to bring back the output voltage to its required Dc level after a sudden change in the source or load conditions.

The above four factors in the conversion process : efficiency, ripple, regulation, and settling time express the operating characteristics of the conversion process and are part of the external specifications when a converter is designed. One should add the three major physical characteristics of a converter : weight , size, and cost which also have to be included in the design problem. Hence, there are seven important parameters in all and the design problem can be stated on the basis of these seven parameters as follows : Given a set of external specifications for the four operating characteristics of the conversion process , chose a method of conversion and technology that minimizes the physical characteristics of the converter which ~~***~~ satisfies all the operating specifications. This design problem is further complicated by the fact that the three physical parameters of the converter ~~don~~ not usually have equal weights. In space related activities weight and size

are supreme, while in commercial applications the cost is the overriding factor. In order to solve the general design problem, as in all engineering design problems, the effect of the choice of methods and the change of operating characteristic values on the physical parameters have to be known.

The approach to this design problem in the past could not account for the general case. There are a large number of papers that deal with the realizability or the theoretically stable operation of converter-like feedback systems (See for example Ref. 1-5). The major thrust in these papers is the evaluation of conditions for the absolute stability of theoretical models that approach pulse modulated converter circuits. In most cases one finds absolute stability criteria too restrictive. There are also excellent papers which illuminate the power conversion field in general. (See for example Ref. 6) . And then there are papers which deal with specific converters and their design (Refs 7-9) . In these later papers a particularly successful Dc-to-Dc converter configuration is discussed which is based on pulse modulation. Still, there is a gap in our knowledge between the very general and the very specific.

It is of course impossible to examine all the presently known conversion methods (and the ones yet to come) and evaluate the effect on the physical characteristics of converters when their operational characteristics are manipulated. For this reason a somewhat different approach is proposed. We shall choose one fundamental and if possible, simple class of Dc-to-Dc power converter methods, which are known to be stable and reliable and allow the manipulation of all four operating characteristics of the conversion process. We shall analyze this class of converters in order to gain insight into the basic principles and mechanisms which could form the basis of sound design. We shall establish criteria that will insure the successful operation of the converter under all external conditions. Then, finally, we shall evaluate the physical parameters of converters that are built on the basis of our

earlier analysis.

The above plan is a long range plan. The first attempt in following this research plan is described in this paper. The class of Dc-to-Dc converters is chosen and described. Attention is paid to the small signal stability, or what is better known as the necessary conditions on the stability of this class of converters. While the method is described, data for two of the operational characteristics, ripple and regulation are obtained. The other two parameters, and the unconditional stability question remain to be solved later.

The converter model is constructed from well described functional blocks. The advantage of this approach lies in the present state of technology, when the most reliable design is built on prepackaged functional modules. It is also emphasized throughout this paper that the method chosen is kept as simple as possible. The simplest method is chosen in the described class of converters which exhibits all the known operating characteristics of realizable power converters.

Only the major details of this research is described in this paper and some examples of the complete design curves are given. A more complete set of curves and all details can be found in a NASA report which is under preparation.

II. THE ONE-LOOP SERIAL BOOST DC-TO-DC CONVERTER

Probably the most direct and simplest Dc-to-Dc converter configuration is shown on Fig. 1. This circuit is known as the serial boost circuit. The Dc power source voltage e_s is turned into a chopped or alternating wave form e_{in} , which is applied to the input of a second order low-pass filter. The diode assures current continuity when the switch is open. The required output Dc voltage level is e_{ref} . Sensing this reference voltage, the output voltage of the converter e_{out} and the input voltage to the filter e_{in} , a yet unspecified control element turns the switch ON and OFF in some manner and insures that the average of the output voltage e_{out} remains close to the required output voltage, e_{ref} .

On Fig. 1. we have shown an idealized filter; therefore, the only dissipative element in the output circuit is the load resistance R_{load} . The input voltage to the filter alternates between two voltage levels, e_{on} and e_{off} , the first arises from the source voltage and the switch voltage drop, while the second is the diode voltage drop. If the resonant frequency of the low-pass filter $\omega_0 = 1/\sqrt{L \cdot C}$ is much smaller than the switching frequency of the switch controller then the output voltage will have small ripple content, as shown on Fig.1. Since the filter has no losses in this idealized model, the average of the output voltage is equal to the average of the input voltage to the filter. The time periods T_{on} and T_{off} (while the switch is held ON or OFF) are controlled by the switch controller and in the general case both could be controlled independently. The frequency of the input voltage to the filter thus becomes: $f = 1/(T_{on} + T_{off})$, or the inverse of the period of switching, $T = T_{on} + T_{off}$.

Since the average input voltage to the filter has to be equal to e_{ref} (because no losses are assumed in the filter), the duty cycle, for which we shall use the greek letter δ ,

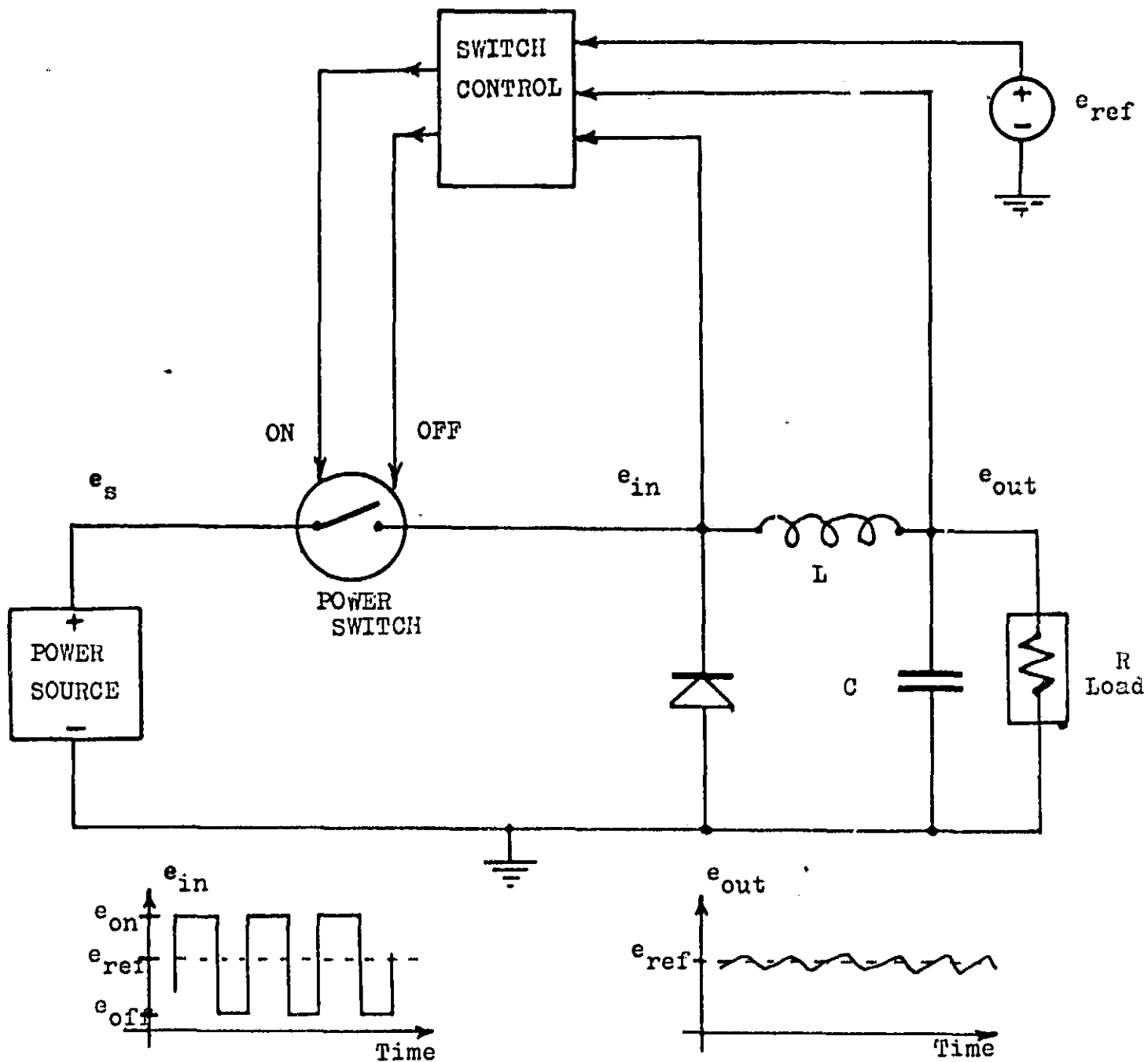


Figure 1. Model of a Serial-Boost Dc-to-Dc Power Converter.

has a simple relationship to the voltages e_{on} , e_{off} , and e_{ref} :

$$\delta = T_{on} / (T_{on} + T_{off}) = (e_{ref} - e_{off}) / (e_{on} - e_{off}) \quad (1)$$

and similarly :

$$1 - \delta = T_{off} / (T_{on} + T_{off}) = (e_{on} - e_{ref}) / (e_{on} - e_{off}) \quad (2)$$

Equations (1) or (2) express the fundamental operation of the converter, which can be stated as follows: Keeping the switch frequency much higher than the filter resonant frequency, adjust the duty cycle of the power switch to the value which produces an average output voltage equal to e_{ref} . In case the source voltage changes, or the diode voltage is a function of the diode current (and the output power), the converter controller can adjust the duty cycle to correct for these changes. There is no real restriction on the switching frequency except that it should be much higher than the filter frequency; therefore, in the adjustments of the duty cycle the switching frequency might also change.

The duty cycle has only the range between values of zero and one, and the output voltage average , e_{ref} has to stay between the values e_{on} and e_{off} . The range of e_{out} can be changed with a transformer, but here we deal with more the basic model of the converter than its physical realization; therefore, we will not discuss the problems associated with including transformers in the output circuit.

Since we know, that for the idealized filter the average of e_{in} is equal to the average of e_{out} , only e_{in} has to be sensed by the switch controller. The circuit shown on Fig. 2. details the switch controller one step further. The heart of the controlling feedback circuit is the integrator with a possible constant gain factor, K_1 . This circuit is much better defined than the general controller on Fig. 1. The general threshold sensor shown on Fig.2. has only one input , e_{cont} . The function

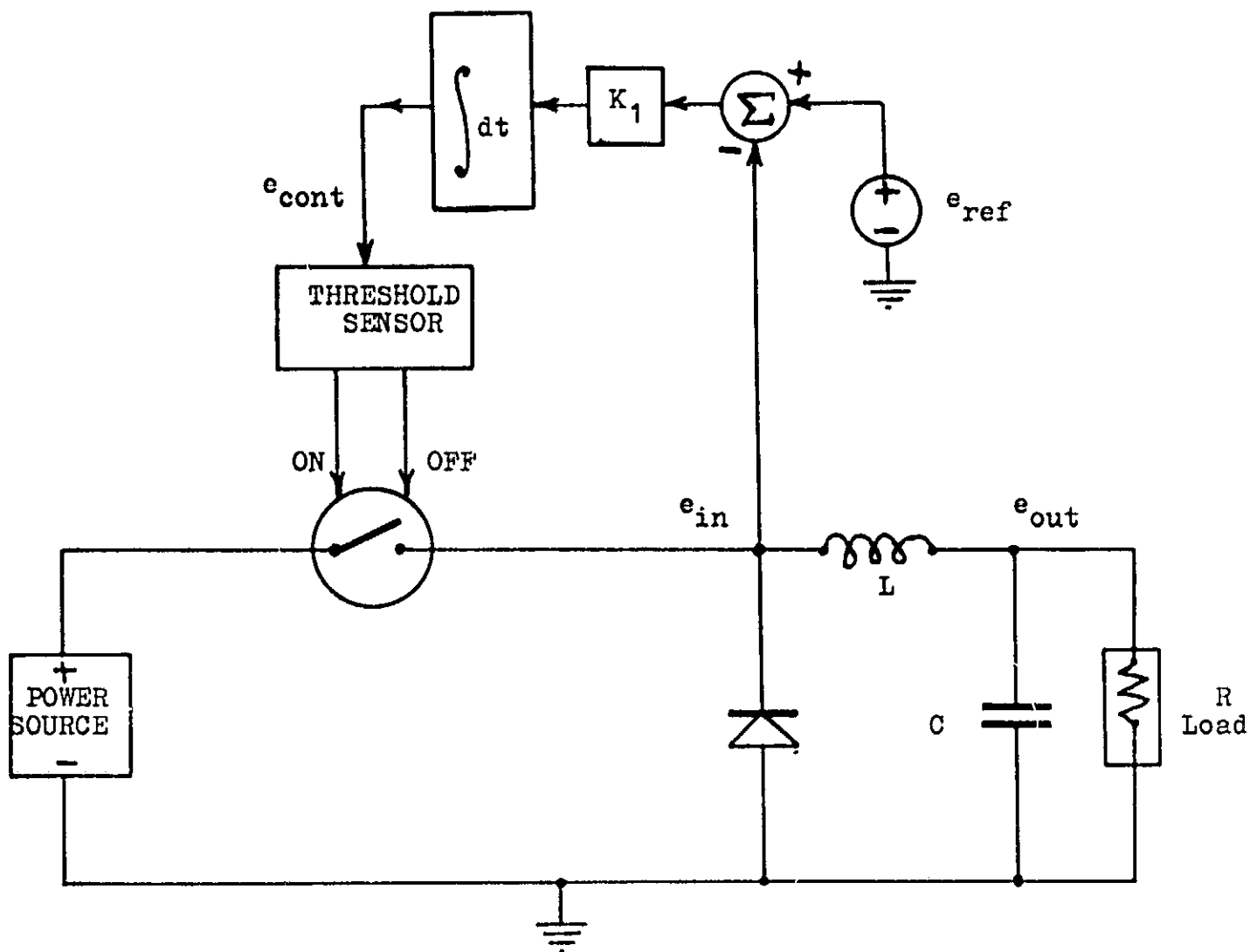


Figure 2. Serial-Boost Circuit with Single Loop Control.

of the threshold sensor is to issue commands to the power switch for turning it ON or OFF. The commands are controlled by the voltage level of the input, e_{cont} . We will demonstrate that the detailed control law for switch control is not needed for the general discussion on the successful operation of the converter because we shall define "successful operation", or stability of the converter in general terms. We simply state that successful operation of the converter is achieved when for a fixed set of voltages e_{on} , e_{off} , and e_{ref} , the converter switch operation is simply periodic with period T , and hence the chopped wave form, e_{in} is also a simply periodic function of time. And absolute stability is defined as the criterium that after a sudden change in the values of e_{on} , e_{off} , and/or e_{ref} , the converter might go through a transition of non-periodic behaviour, but settles again to a simply periodic operation. It is important to emphasize the above statement, because the converter feedback system is complicated enough to exhibit many different kinds of periodic behaviour which are not simply periodic. The only unique periodic behaviour is the simply periodic behaviour and we shall define the "stable" operation of the converter around it.

Now our task is to devise a simple threshold sensor scheme that insures the absolute stability of the converter according to our definition above. Before we show the three major forms of threshold sensor designs it is worthwhile to demonstrate here that simply periodic behaviour of the circuit on Fig. 2. is indeed sufficient to ensure the correct converter output. All signals are simply periodic; therefore, the integrator output voltage, e_{cont} must satisfy the following equality:

$$e_{\text{cont}}(t+T) = e_{\text{cont}}(t) \quad (3)$$

where t is any time and T is the period of operation. The input to the integrator is $K_1 \cdot (e_{\text{ref}} - e_{\text{in}})$ and we can evaluate the value $e_{\text{cont}}(t+T)$ as follows :

$$e_{\text{cont}}(t+T) = e_{\text{cont}}(t) + K_1 \cdot \int_t^{t+T} (e_{\text{ref}} - e_{\text{in}}) \cdot dt \quad (4)$$

and therefore from Eqs. (3) and (4) we have :

$$\int_t^{t+T} (e_{\text{ref}} - e_{\text{in}}) \cdot dt = 0 \quad (5)$$

Since e_{ref} is a constant (or can be assumed to be a constant for one period of operation), we get from Equ.(5) :

$$e_{\text{ref}} = (1/T) \int_t^{t+T} e_{\text{in}} \cdot dt = \bar{e}_{\text{in}} \quad (6)$$

where the bar over e_{in} indicates time average. Equation (6) states that the time average of the filter input voltage is equal to e_{ref} , and with no losses in the output filter, the time average of the output voltage is also equal to e_{ref} .

We shall now specify the threshold sensor operation. We have chosen the three major methods used in practice. Two of these methods have duals; therefore, there will be five different methods of threshold sensor operation. Since all methods have to adjust the duty cycle to the value shown on Eqs. (1) or (2), they are basically different in handling the overall frequency of operation $f = 1/T$. The dual methods are characterized by the important behaviour that in the equations which describe the dual method operation the duty cycle factor, δ , is replaced by the factor $1-\delta$. The significance of this simple relationship will be shown later.

II.1. Free-Running Threshold Sensor

The operation of the free-running threshold sensor method is outlined on Fig. 3. There are two thresholds for this method, called e_{TH1} and e_{TH2} . When the control voltage, which is the input voltage to the threshold sensor reaches e_{TH1} or exceeds e_{TH1} , the sensor issues commands to the power switch and turns it ON. When e_{cont} reaches the other threshold

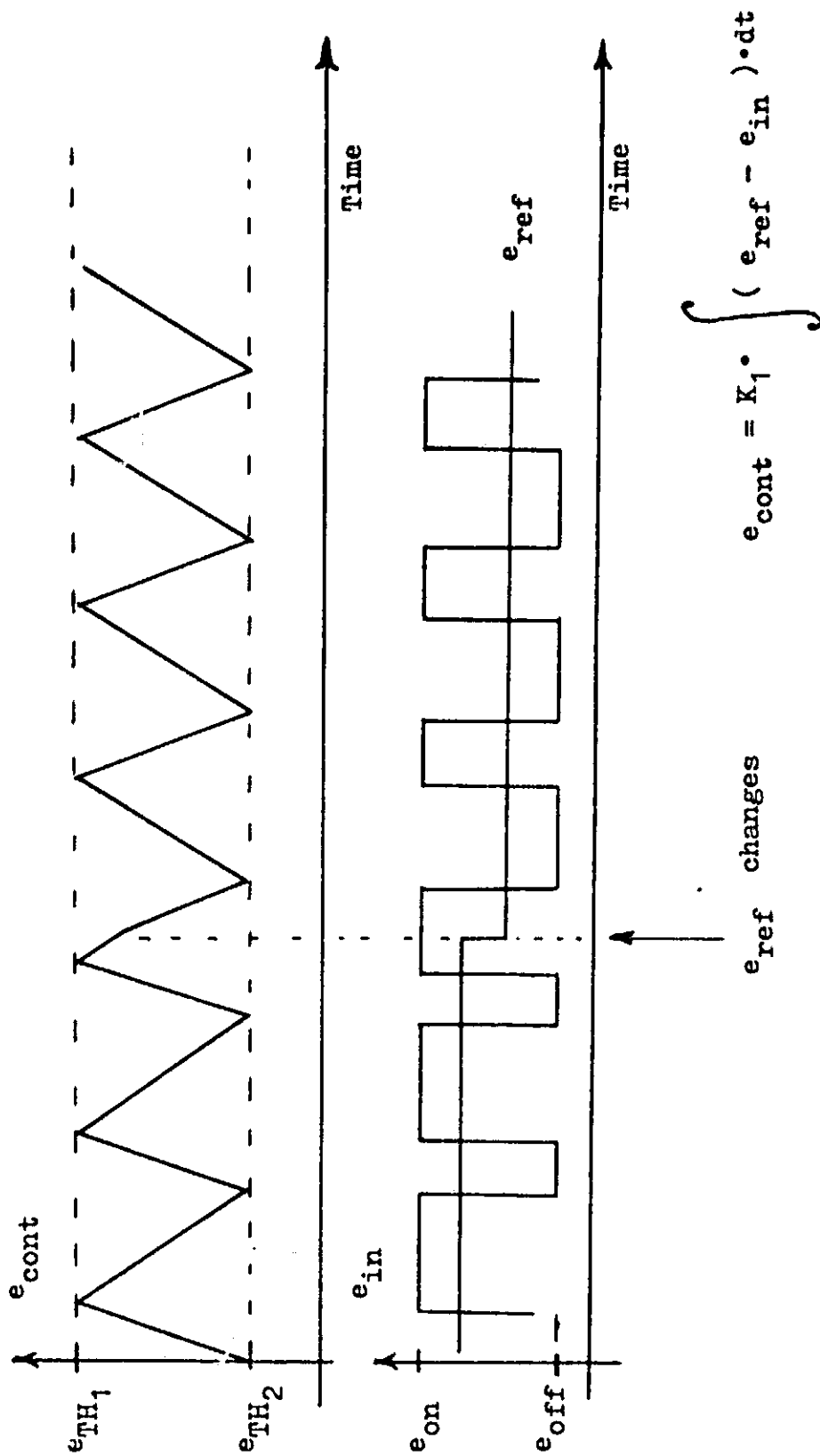


Figure 3. Free-Running or Two-Threshold Threshold Sensor.

value, e_{TH2} , or stays below e_{TH2} , then the sensor issues commands to the power switch to turn it OFF. When the converter reaches stable operation, the input voltage to the sensor, e_{cont} remains between e_{TH1} and e_{TH2} . When the switch is ON the input to the integrator is $e_{ref} - e_{on}$, which is negative; and when the switch is OFF the input to the integrator is $e_{ref} - e_{off}$, which is positive; therefore, the integrator output is a triangular waveform. (See Fig. 3.). We also show on Figure 3. what happens after a sudden change in the reference voltage. In one period of operation the converter returns to its periodic, or stable operating mode.

If the reference voltage is a constant, and we use the letter Δ for the difference between the two threshold levels: $\Delta = e_{TH1} - e_{TH2}$, we can express T_{on} and T_{off} time intervals:

$$\begin{aligned} T_{on} &= (\Delta / K_1) / (e_{on} - e_{ref}) & \text{and} \\ T_{off} &= (\Delta / K_1) / (e_{ref} - e_o) & \text{seconds} \end{aligned} \quad (7)$$

Now we substitute Eqs. (1) and (2) into Equation (7) and express the operating frequency: $f = 1 / (T_{on} + T_{off})$, we get:

$$f = (K_1 / \Delta) \cdot \rho \cdot (1 - \rho) \cdot (e_{on} - e_{off}) \quad (8)$$

Equation (8) shows that the frequency of operation is not only a function of the circuit parameters Δ , and K_1 , but also ρ , the duty cycle. In a later section we will present curves which will be based on the parameters of frequency and duty cycle. It will be important to realize when these curves are applied to the free-running case, that these two parameters are not independent but are related by Equ. (8).

The dual mode of operation of the free running case becomes the same as its basic operation. This fact is demonstrated

by Equ. (8) because replacing φ by $(1-\varphi)$ does not change Equ.(8). Equation (8) and in fact all controlling equations for the free-running case are symmetrical for the replacement of φ by $(1-\varphi)$.

From a practical point of view the threshold sensor of the free-running mode can be realized with two comparator circuits and a power switch that can be turned ON and OFF by voltage control. The control voltage of the power switch can be manipulated by the outputs of the two comparators that signal when the input voltage reaches or exceeds e_{TH1} , or reaches or stays below e_{TH2} .

II.2. Synchronized Threshold Sensor

The operating mode of the synchronized threshold sensor is outlined on Figure 4. The threshold sensor includes a clock which generates pulses periodically, with period T . There is only one threshold level, e_{TH2} , whose function is the same as e_{TH2} in the free-running case; it turns the power switch OFF when the control voltage reaches e_{TH2} or stays below e_{TH2} . The clock pulses are used to turn the power switch ON. Hence, the turning ON function is synchronized to an external clock.

The frequency of the operation of the converter is thus constant. However, the individual times T_{on} and T_{off} are variables and are used to adjust the duty cycle to its proper value. As shown on Fig. 4. the control voltage e_{cont} at the time the switch is turned ON is not fixed, as in the free-running case. Let us designate the control voltage at the "n"th clock pulse as $e_{cont}(n)$, then we can express again T_{on} and T_{off} as follows :

$$\begin{aligned} T_{on} &= (e_{cont}(n) - e_{TH2})/K_1 \cdot (e_{on} - e_{ref}), \text{ and} \\ T_{off} &= T - T_{on} \end{aligned} \tag{9}$$

where, T the period of the clock is a constant.

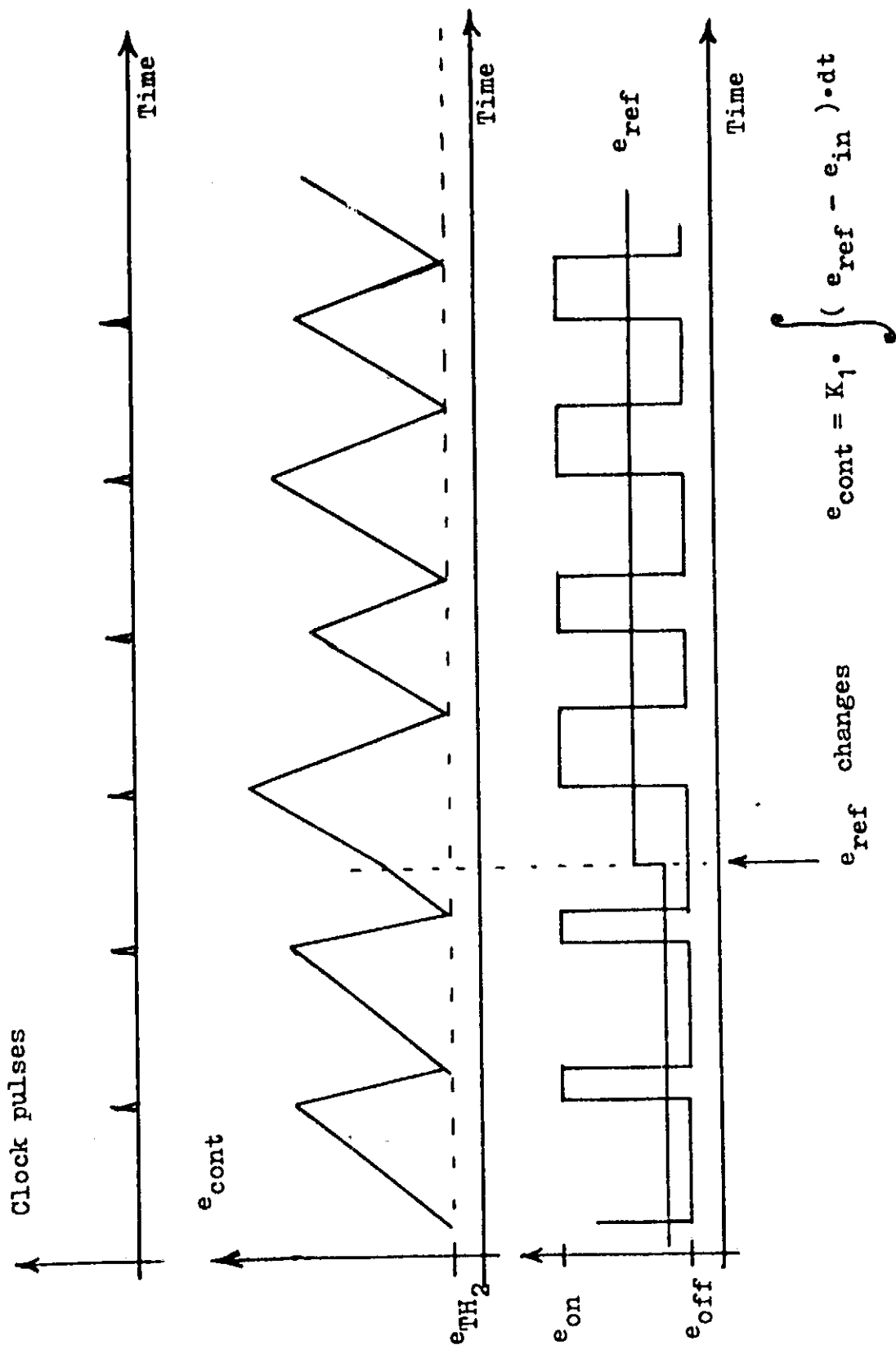


Figure 4. Synchronized Threshold Sensor (Synchronized ON control)

It might be concluded from Equ. (9) that T_{on} and T_{off} are not functions of the voltage e_{off} , but this is not the case because the control voltage at the next clock pulse (the $n+1$ 'th) is a function of the voltage e_{off} :

$$e_{cont}(n+1) = e_{TH2} + T_{off} \cdot (e_{ref} - e_{off}) \quad (10)$$

On Figure 4. the behavior of the control voltage is shown after a sudden change occurs in the reference voltage. The successive values of the control voltage at the successive clock pulse times are not constant. It is not even obvious that the controller settles down to a periodic operating mode. We can examine this question of stability by substituting Equ. (10) into Equ. (9) and thus expressing the control voltage at the $n+1$ 'th clock pulse time in terms of the control voltage at time of the n 'th pulse:

$$e_{cont}(n+1) = K_1 \cdot T \cdot (e_{ref} - e_{off}) + e_{TH2} - (e_{cont}(n) - e_{TH2}) \cdot (e_{ref} - e_{off}) / (e_{on} - e_{ref}) \quad (11)$$

which can also be expressed in terms of the duty cycle, using Eqs. (1) and (2) :

$$e_{cont}(n+1) = e_{TH2} / (1 - \rho) + K_1 \cdot T \cdot \rho \cdot (e_{on} - e_{off}) - \left[\rho / (1 - \rho) \right] \cdot e_{cont}(n) \quad (12)$$

In order to look for stability, let us replace the control voltage $e_{cont}(t)$ with its equilibrium value at the n 'th clock pulse and a variable, $\epsilon(t)$ which expresses how far the control voltage is from its equilibrium value. Since at equilibrium the control voltage is periodic, we can find the equilibrium value, which we will designate as e_0 , by substituting this into the place of $e_{cont}(n)$ and $e_{cont}(n+1)$ in Equation (12). We get :

$$e_0 = e_{TH2} + K_1 \cdot T \cdot (e_{on} - e_{ref}) \quad (13)$$

and we also have :

$$\epsilon(n) = e_{cont}(n) - e_0 ; \quad \epsilon(n+1) = e_{cont}(n+1) - e_0 \quad (14)$$

Finally, we can substitute Eqs. (13) and (14) into Equ. (12) and get :

$$\epsilon(n+1) = -\left[\rho / (1 - \rho)\right] \cdot \epsilon(n) \quad (15)$$

We made no specific assumptions during the manipulation of these equations, and the advantage of having the equation in the form of Equ. (15) is that it expresses stability on the basis of our definition in the last section, on the basis of a simply periodic solution of the equations. The variables in the above equation, $\epsilon(n)$ and $\epsilon(n+1)$ are related by a difference equation. The magnitude of the variable at any time expresses the difference between the equilibrium or periodic solution and the actual solution, therefore the variable $\epsilon(t)$ must approach zero for stable operation of the converter. This occurs only if the magnitude of the multiplying factor of $\epsilon(n)$ in Equation (15) is less than unity; which is equivalent to the condition that :

$$\rho < 0.5 \quad (16)$$

We conclude that the synchronized threshold sensor will operate only for duty cycles of less than .5 and becomes unstable for duty cycles larger than .5 .

We have not discussed the dual case until now. The dual case has one threshold, e_{TH1} , which turns the power switch ON, and an external clock which turns the switch periodically OFF. All equations described for the synchronized case above are valid for the dual synchronized case with suitable substitution of the value e_{TH1} in place of e_{TH2} , and $1 - \rho$ in place of ρ . The later substitution is important because

it indicates that for the dual synchronized case Equ. (15) becomes :

$$\epsilon_{(n+1)} = -\left[(1-\rho)/\rho\right] \cdot \epsilon_{(n)} \quad (17)$$

therefore the dual synchronized case is only stable for duty cycles larger than .5 .

We can conclude that synchronized or clock driven threshold sensor converters can be built only for the half range of duty cycles. One will work for duty cycles : $0 \leq \rho < .5$, the dual method will work for $.5 < \rho \leq 1$, but neither will work for the entire range of duty cycles. Another important difference between the synchronized converter and the free running converter is in their behavior after a sudden change in input voltages. As shown on Figs. 3. and 4. , the synchronized converter does not recover in one switching period as the free-running converter , but the control voltage oscillates around its equilibrium state. This also can be concluded from Equ.(15) which shows that any disturbance will decay as a geometric series with multiplicative constant $[-\rho/(1-\rho)]$, (~~not~~ $[-(1-\rho)/\rho]$ for the dual case).

From a practical point of view , only one comparator circuit is needed for the synchronized threshold sensor but an external clock or a built in astable multivibrator is also necessary. Again, the power switch would have to be controlled by voltage control.

II. 3. The Constant On-Time Threshold Sensor

The third method for the threshold sensor is outlined on Figure 5. Only one threshold level is used, e_{TH1} , which, as before, is used to turn the power switch ON whenever the control voltage reaches this level, or goes above the threshold level. After the switch turns ON it will stay ON , regardless of the control voltage for a given constant time, T_{on} . After this time period the switch turns itself OFF . If the control voltage is above e_{TH1} then the switch is turned ON again,

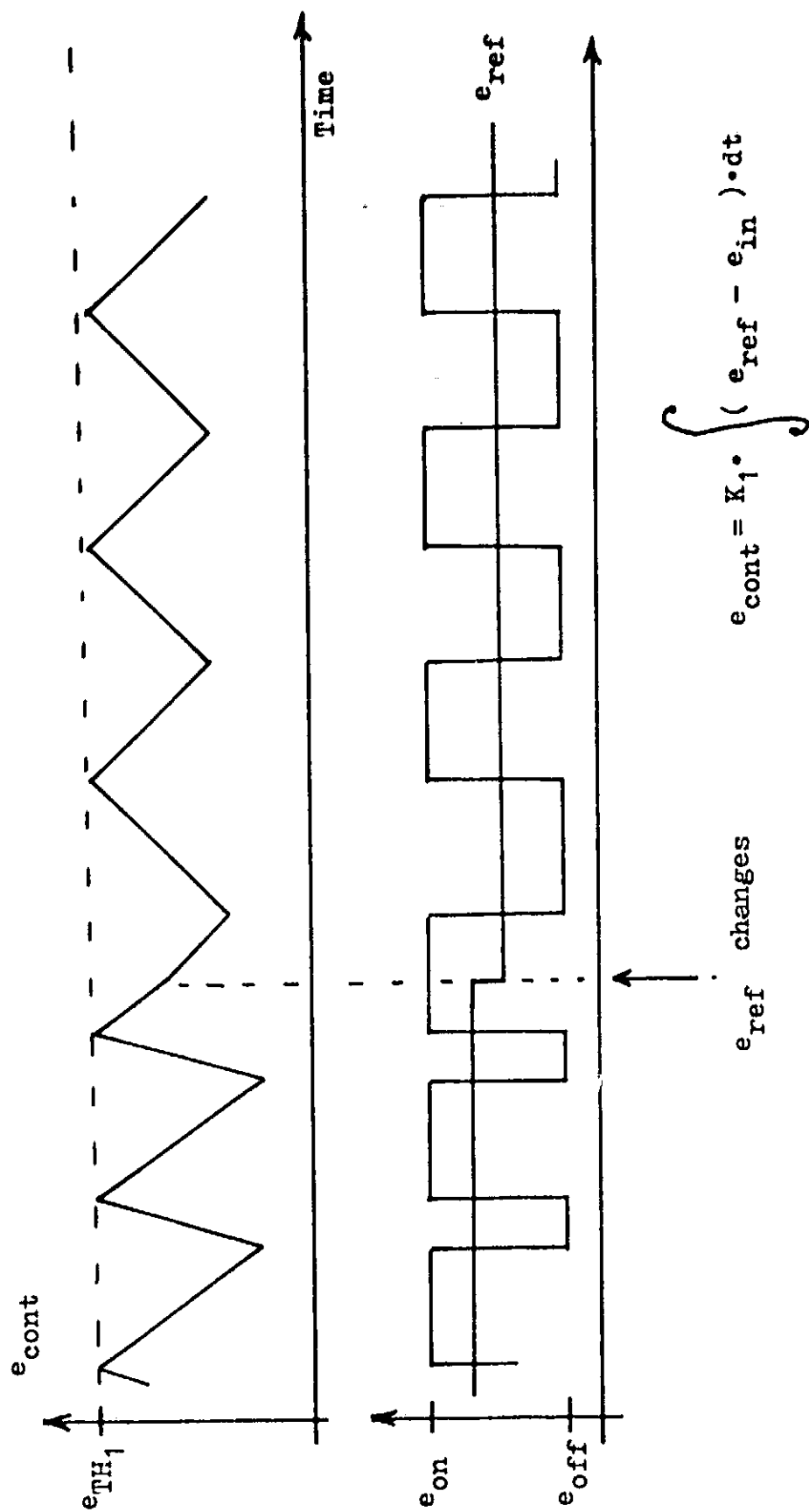


Figure 5. Constant ON-Time Threshold Sensor.

otherwise the switch stays in the OFF position until the control voltage reaches the threshold level e_{TH1} again.

The frequency of operation of this type of converter depends directly on the duty cycle. The time the switch is in the OFF position is simply : $T_{off} = [(1-\rho)/\rho] \cdot T_{on}$, and the frequency of operation is :

$$f = (1/T_{on}) \cdot \rho \quad (18)$$

We see that the frequency of switching is directly proportional to the duty cycle. This relationship is also very important when general curves are interpreted which are given in terms of the frequency and duty cycle as parameters.

As shown on Fig. 5. , the equilibrium operating conditions are reached within one switching period after a sudden change in the reference voltage. The converter can also be used for the whole range of duty cycles, at least in theory. In practice, since the frequency is directly proportional to the duty cycle, there would be some limitations on the values of the duty cycle that could be used. We can also evaluate the swing of the control voltage for a given set of input voltages :

$$e_{cont}(\min) = e_{TH1} - K_1 \cdot T_{on} \cdot (e_{on} - e_{ref}) \quad (19)$$

where $e_{cont}(\min)$ refers to the minimum of the control voltage after the converter reached its stable operating mode. This minimum occurs when the switch turns itself OFF , (See Fig.5.).

The dual case for this control mode is the constant T_{off} mode, when the threshold level is e_{TH2} , and is used to turn the power switch OFF. The normal position of the switch is ON for this dual case, and when the control voltage reaches e_{TH2} the switch is turned OFF and then it stays OFF for a given period of time , T_{off} . Again, the equations are similar, with

the suitable substitutions of e_{TH2} and $(1-\rho)$ into the equations of the constant T_{on} case. Without derivation we give the frequency of the dual converter :

$$f_{dual} = (1/T_{off}) \cdot (1 - \rho) \quad (20)$$

From a practical point of view, this method uses one comparator circuit and possibly one one-shot multivibrator, which times the period for which the switch stays ON. On the other hand, the power switch might be constructed in such a way that once turned ON, it stays ON for a given period of time only. Here lies the importance of this method. The turning OFF of the power switch could be current controlled rather than voltage controlled, hence this method of threshold sensor could be applied to circuits for which there are no voltage controlled power switches available. When, in the future, we shall deal with the physical characteristics of this type of converters, this unique quality of the constant T_{on} control will take on added importance.

We have now concluded the discussion on the one-loop converter threshold sensor schemes. We have presented five distinct methods, which should be sufficient for most physical requirements. The first method varied both T_{on} and T_{off} and also the frequency of operation of the converter, the second method kept the sum $(T_{on} + T_{off})$ constant, while adjusting the ratio of T_{on} to T_{off} , and the third method adjusted T_{off} only, while keeping T_{on} constant. As long as we search for simple methods, these five methods are exhaustive enough. And as long as the average of the output voltage is equal to the average of the input voltage to the filter, we have solved the stability problem for all these cases and we could stop our analysis here. This is so, because we ensured that the average of e_{in} in all these five cases for the stable operating modes of the converter is equal to e_{ref} , the reference voltage.

However, real filters are not lossless. Inductors always carry resistance and at high frequencies capacitors have losses also. Power loss in the output filter will cause the average of the output voltage to be less than the average of the input voltage to the filter. Until now we have been keeping the average of the filter input voltage a constant and equal to the reference voltage. Under these conditions the Dc output voltage will be the function of the power delivered to the load and we have poor regulation.

Since regulation is one of the operating characteristics, we should be expected to control regulation for a practical converter. Therefore, the outlined five methods in this section are not sufficient yet for converter design. We shall show in the next section how the addition of a second feedback loop solves the problem of regulation and at the same time causes the problem of instability.

III. THE TWO-LOOP SERIAL BOOST DC-TO-DC CONVERTER

It was mentioned in the previous section that in practical converters the output voltage does not have the same time average as the filter input voltage because of losses in the filter. Therefore, the output voltage has to be sensed as well as the filter input voltage for accurate output voltage control. We have again adopted the simplest method of introducing into the feedback loop the output voltage. We show the resulting two-loop serial boost converter circuit on Figure 6. The structure of the main feedback loop has not changed. The methods of threshold sensor are the same as before. But the input voltage to the threshold sensor, e_{cont} has a component in it that includes the voltage difference $(e_{ref} - e_{out})$ multiplied by a constant gain factor K_2 . We have stated that the second loop was needed to improve regulation. Let us show how this second loop effects the regulation of the converter.

We shall compare the regulation of the two-loop converter to that of an equivalent one-loop converter. We can always recover the one-loop converter from the two-loop converter by setting K_2 to be zero. Therefore we shall express regulation in terms of K_2 and compare the regulation of the converter for different values of K_2 to that when the second loop gain, K_2 is set to be zero.

We shall keep the filter characteristics constant. Let us assume that at maximum loading the average output voltage is "r" times the average input voltage to the filter :

$$\bar{e}_{out} = r \cdot \bar{e}_{in} \quad (21)$$

where "r" could be thought of as a loss factor, and the bars indicate time average. The loss factor, r , is always smaller than one and it is a direct measure of the quality of the

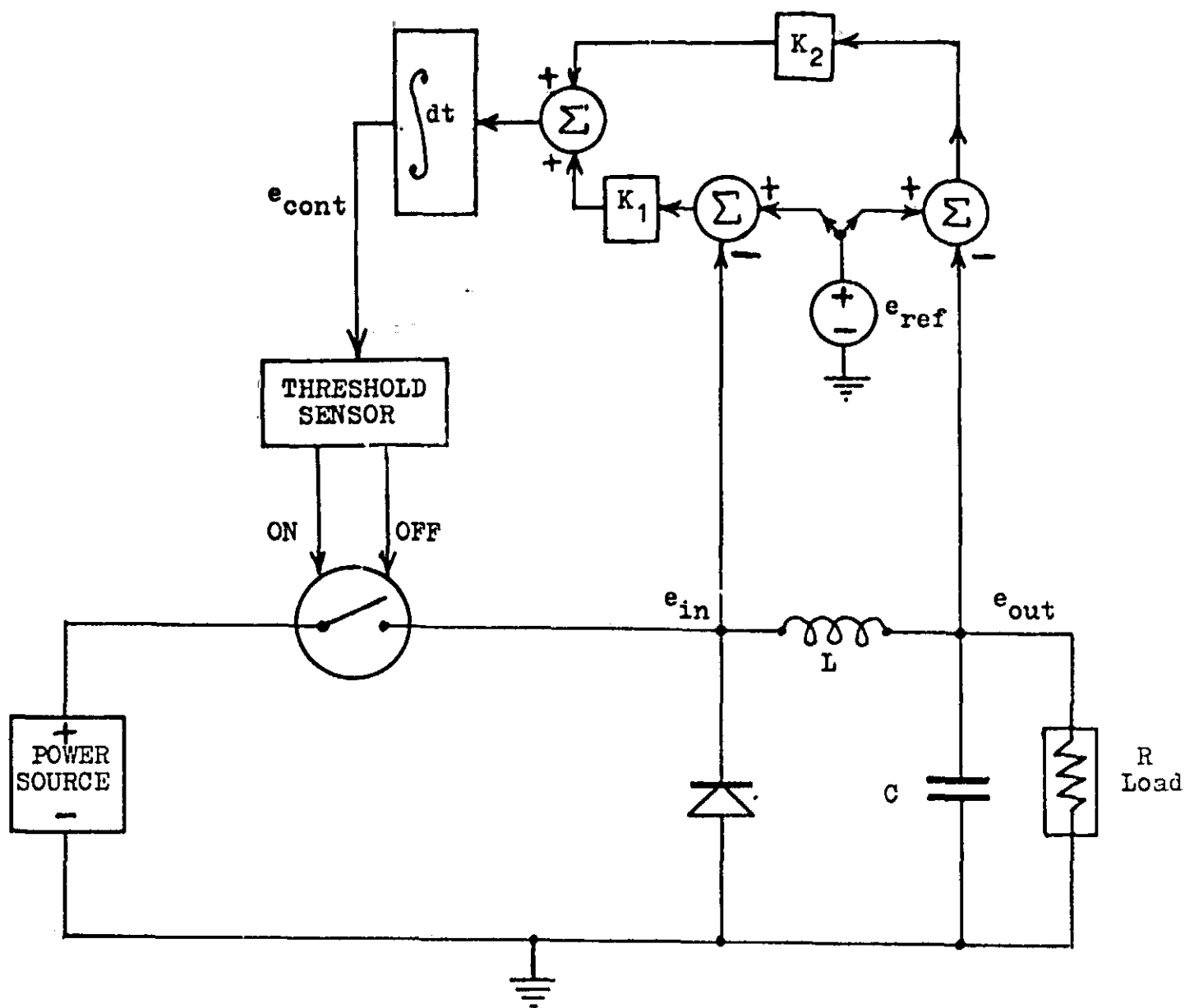


Figure 6. Serial-Boost Circuit with Double-Loop Control.

output filter. Similarly to the derivation of Equ.(3) to Equ.(6) we can express the control voltage for one period of operation :

$$e_{\text{cont}}(t+T) = e_{\text{cont}}(t) + \int K_1 \cdot (e_{\text{ref}} - e_{\text{in}}) + K_2 \cdot (e_{\text{ref}} - e_{\text{on}}) \cdot dt \quad (22)$$

and because the voltage e_{cont} is simply periodic with period T the integral in Equ.(22) has to be zero. Since e_{ref} can again be assumed to be constant for one period of switching, the evaluation of Equ.(22) gives us :

$$(K_1 + K_2) \cdot e_{\text{ref}} = K_1 \cdot \bar{e}_{\text{in}} + K_2 \cdot \bar{e}_{\text{out}} \quad (23)$$

where again the bars indicate time averages. Substituting Equ.(21) into Equ.(23) results in the following equation :

$$\bar{e}_{\text{out}} = (1 + K_2/K_1) / (1/r + K_2/K_1) \cdot e_{\text{ref}} \quad (24)$$

If we define regulation by the ratio of the difference between the no load output and the maximum load output dc voltages to the nominal output voltage , e_{ref} , and observe that at no load the output voltage average is equal to e_{ref} , we get :

$$\text{Regulation} = \frac{1 - r}{1 + r \cdot (K_2/K_1)} \quad (25)$$

Equation (25) shows that for the single-loop converter regulation is equal to $1-r$, while for very large ratios of K_2/K_1 the regulation approaches the expression $(1-r)/(r \cdot K_2/K_1)$. The loss factor , r is a filter characteristics. The regulation of the converter , on the other hand , could be specified by the designer. If the value of r is for example .9 but the designer requires a regulation of .01 then the value of K_2/K_1 should be at least 11. Thus , Equation (25) places a lower limit on the ratio K_2/K_1 when the filter and the required regulation are fixed. In fact,

one can achieve as good of regulation as one requires by setting the ratio K_2/K_1 high enough. But large feedback gains cause instability and there will be an upper limit to this ratio for insuring the stable operation of the converter. The question of at least one kind of stability of the converter will be discussed in the next section. But before closing this section we shall discuss a normalization procedure that will greatly reduce our number of variables when the stability question is analyzed.

III.1. Normalization Procedure for the Two-Loop Converter.

Our final aim is to provide curves that are useful to a converter designer. Until now we have dealt with a large number of physical variables, like e_{on} , e_{off} , e_{ref} , K_1 , K_2 , and filter components L , C , R_{load} , and loss factor r . In order to make the designing curves as general as possible, we will present them in normalized form. All variables used to produce these curves will be dimensionless similarly to filter design problems in electronics. For the designer it is important to know this normalization procedure, in particular how one can calculate the values of the normalized parameters from physical variables.

One of the most important dimensionless parameter of the converter is the ratio of the switching frequency to the resonant frequency of the output filter. We have seen that ripple of the output depends significantly on this parameter. We shall define this normalized frequency, ν , by the following equation:

$$\nu = 2\pi\sqrt{L \cdot C} / T \quad (26)$$

where L and C are the inductor and the capacitor values in the output filter, and T is the switching period of the converter in seconds. How the period of switching is connected to the physical variables of the converter has been discussed in the previous section.

Another important normalized parameter is the damping ratio that expresses the loading factor of the output filter. The damping ratio, for which the greek letter will be used : η , is expressed by the filter component values L and R :

$$\eta = L / 2 \cdot R_{load} \quad (27)$$

We have already introduced the duty cycle which is another normalized parameter of the converter. The duty cycle , δ , which is defined as $T_{on} / (T_{on} + T_{off})$ can be also defined by the voltage levels to the input filter (See Eqs. (1) or (2)) .

Finally , it can be shown that not both feedback gains are needed for the normalized model but only their ratio, K_2/K_1 . This is so because once the filter resonant frequency and the switching frequency are fixed, K_1 would have to be adjusted for giving the required value to ν , the frequency ratio. The ratio of gains K_2/K_1 will simply be called , K , normalized gain. We have already shown , that the normalized gain , K , plays an important part in reducing regulation error, and we will show shortly that it plays an important role in the stability of the converter.

Table I. summarizes the four normalized parameters that define the two-loop serial boost converter. We have not included the loss factor of the output filter , r , in these four basic parameters, because this factor will not influence our subsequent work. It is this loss factor, however , which necessitates the inclusion of the second loop, and with it the second loop parameter , K , the normalized gain. The other three parameters : ν , η , and δ , are also parameters of the one-loop converter and influence the operating characteristics of the one-loop converter - as for example - the output ripple.

SYMBOL	PARAMETER NAME	VALUE IN PHYSICAL QUANTITIES	REMARKS
ν	Normalized Frequency	$2\pi\sqrt{L\cdot C}/T$	Ratio of switching frequency to the resonant frequency of the filter.
η	Damping ratio	$L/2\cdot R_{load}$	Loading factor of the output filter.
ρ	Duty Cycle	$\frac{(e_{ref} - e_{off})}{(e_{on} - e_{off})}$	Corrected by the feedback circuit to give correct output.
K	Normalized Gain	K_2/K_1	Ratio of feedback gains. Improves regulation, effects stability.

Table I. Summary of the Normalized Parameters of the Two-loop Serial Boost Dc-to-Dc Converter.

IV. DETERMINATION OF THE SMALL SIGNAL STABILITY OF THE TWO-LOOP SERIAL BOOST DC-TO-DC CONVERTER

We have shown that given some physical voltages e_{on} , e_{off} , and e_{ref} we can build a simple two-loop serial boost Dc-to-Dc converter that will satisfy the requirements placed on the ripple magnitude of the output voltage and the output voltage regulation. We have also shown five separate threshold sensor methods with which this converter can be built. But we have not proved in any sense that the converter will indeed operate in the stable, simply periodic mode. We have not shown or even discussed the possibility that at some converter parameter values the converter might not have a stable operating condition at all. We will be interested now in the so called small signal stability of the converter. Small signal stability means that given a stable operating mode of the converter, when the state of the converter is moved a small amount from its equilibrium state then it will return to its equilibrium state. This condition is a necessary condition for stability, since all physical systems include noise, which necessarily remove the dynamic systems from their equilibrium operating state.

Along with a necessary condition of stability researches look for "sufficient" conditions of stability. The sufficient condition of stability expresses the fact that no matter what initial state the system is in, it will settle to its equilibrium state, which we defined here, as a simply periodic operating mode. The question of large signal stability is: what are the conditions which insure that the converter will not follow large signal oscillations even though it has a stable simply periodic operating state? The converter circuit shown here is grossly non-linear. Even if we ignore the physical realities of saturable amplifiers and integrators, one of the variables, the duty cycle has a finite range, and the threshold sensor circuit cannot be described by linear function elements. So we are faced here with the large signal stability of a grossly non-linear

feedback control system. This is a very complex problem and experience tells us that large signal stability conditions depend significantly on saturating conditions in the physical circuit. Hence, the detailed circuits and voltage levels are necessary to determine large signal stability conditions.

We are suggesting the following solution to this complex problem. Let us find the best possible conditions for which small signal stability exist by ignoring the large signal stability question all together. Without small signal stability there is no stable operating mode. But once the best stable converter configurations are found, we will introduce a method by which we will ensure that the converter will return to the neighborhood of its equilibrium state from any initial state or disturbance. We will introduce a third feedback loop that will deal exclusively with the large signal modes of the converter. The function of this third feedback loop will be to bring back the state of the converter to near its equilibrium state. Small signal stability then will be sufficient to insure stable operation. The introduction of the third feedback loop will be a part of our future work and hopefully will be reported on later.

Now, we can turn our attention to the small signal stability of the converter. We have developed two separate methods of determining small signal stability for the described converter circuits. The first method involved analog computer simulation and was highly succesful. The second method involved analytic perturbation techniques, and while gave results which were used to check the simulation results, it involved too much algebra and digital computer time and therefore was not used extensively. We feel, it will suffice to describe the first method here, and present some selected results for the demonstration of this method's usefulness.

For the analog computer simulation of the converter we have used a special purpose analog computer developed some years ago at the Electronics Research Center of NASA , in Cambridge, Massachusetts. We found it very useful to simplify the two-loop converter circuit on Figure 6. by moving the signal e_{ref} through the summing points , so we get $e_{in}-e_{ref}$ for the filter input voltage and $e_{out}-e_{ref}$ for the output voltage and then normalizing all voltages to the voltage swing which equals to $e_{on} - e_{off}$. Let us call the normalized voltages $v(t)$, then for all voltage signals we have :

$$v(t) = e(t) / (e_{on} - e_{off}) , \quad (28)$$

and in particular :

$$v_{on} = (e_{on}-e_{ref})/(e_{on}-e_{off}) = 1-\rho \quad (29)$$

and

$$v_{off} = (e_{off} - e_{ref}) / (e_{on}-e_{off}) = -\rho \quad (30)$$

The simulated voltage output $v_{out}(t)$ can also be expressed :

$$v_{out}(t) = (e_{out}(t) - e_{ref}) / (e_{on}-e_{off}) \quad (31)$$

which shows that the simulated voltage output's equilibrium value is zero. Also, the swing between v_{on} and v_{off} for the simulated model is always unity which simplifies the simulation of the power switch. Finally, we can move the gain factor K_1 beyond the summing point and through the integrator and include it into the threshold sensor, while in the other branch the gain becomes $K_2/K_1 = K$. The simulated converter circuit is shown on Figure 7. The filter is already shown in a normalized form when both capacitor and inductor have values of unity, and the resistor has the value of 2η .

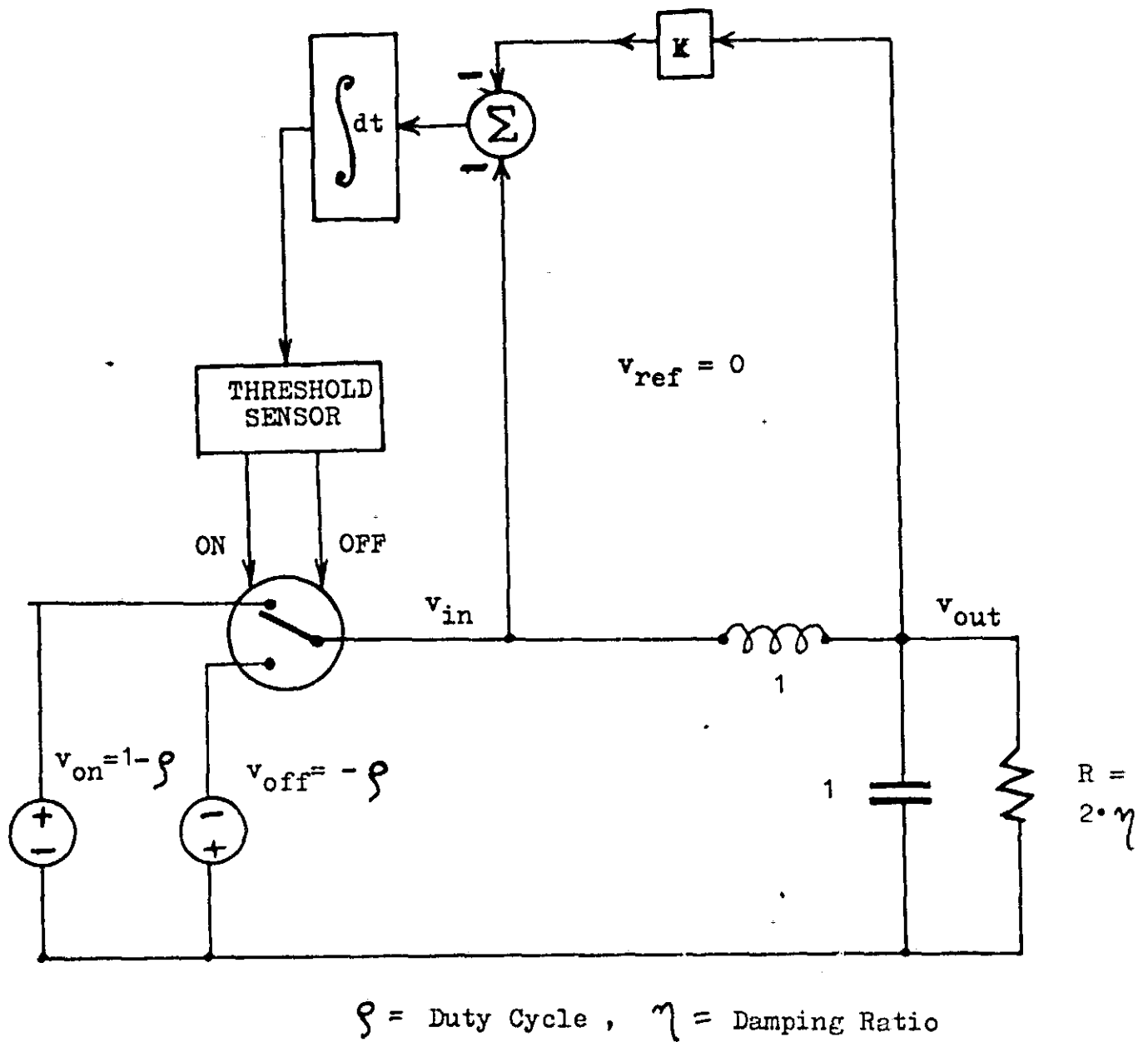
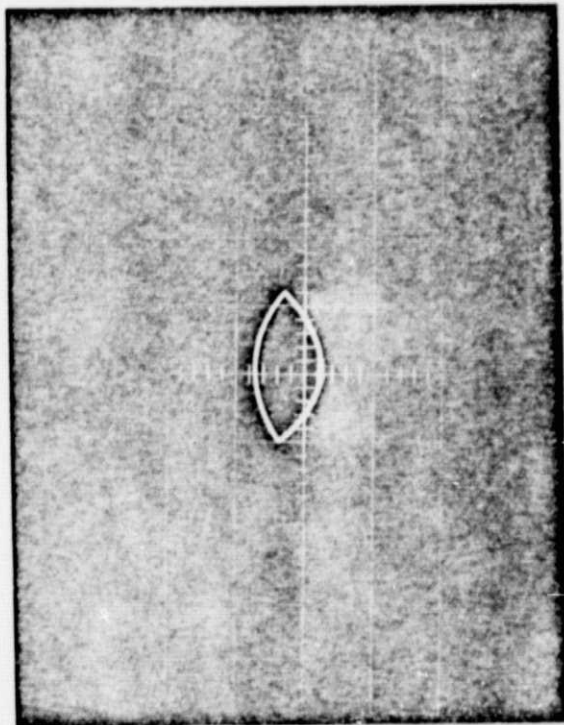


Figure 7. Analog Simulation Model of the Double-Loop Serial-Boost Dc-to-Dc Power Converter.

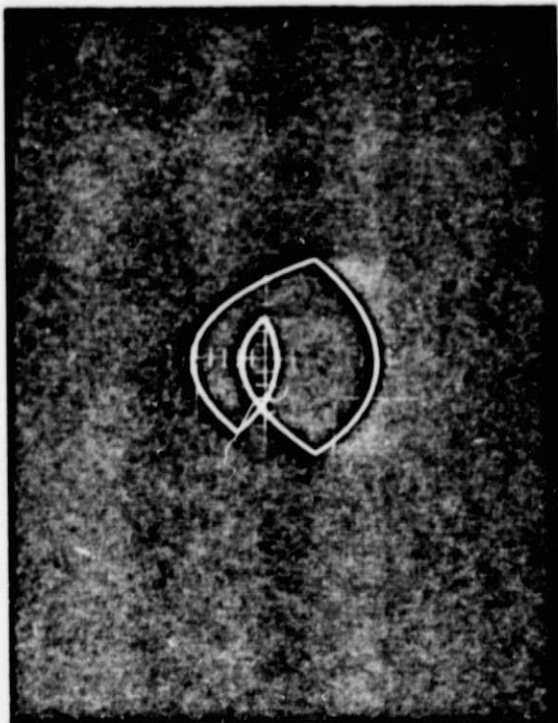
The detailed analog simulator circuits will not be described here, but will appear in a technical report that will include all the details of this research¹⁰. It will suffice to say that two integrator with feedback loops can simulate the low pass filter, while the gain factor and the integrator are standard analog computer elements. The threshold sensor can be also constructed from non-linear circuit elements, such as zener diodes and multivibrators and standard operational amplifiers. For each of the four parameters, ν , η , ξ , and K , precision ten-turn potentiometers were employed. The frequency of the switch was controlled by a gain factor in the threshold sensor circuit and was also manipulated by a ten-turn precision potentiometer.

The determination of the limiting gain K for stable operation was conducted in the following manner: The potentiometers were set for a set of three parameter values, ν , η , and ξ , and then the gain, K was increased from zero to the value which caused instability. The instability was detected by monitoring the output voltage of the simulated converter on the vertical axis of an oscilloscope while using the derivative of the output voltage, dv_{out}/dt for the horizontal axis. This method gave us the maximum sensitivity for detecting instabilities. Since the coordinates are v and dv/dt , we call these outputs on the oscilloscope phase plane curves.

When instability was reached at a given feedback gain, K , the behaviour of the simulated output had quite a variety. Sometimes the instability caused doubly periodic behaviour (See Figure 8), other times the oscillations became large signal and saturated the amplifier circuits. For other operating conditions the pattern never settled down to a fixed pattern, but exhibited relaxation type of oscillations. In all these cases it was not difficult to distinguish between the stable



a.) Stable Converter



b.) Unstable Converter

Figure 8. The Plot of e_{out} vs. $\frac{de_{out}}{dt}$ (Phase plane curve) for Both Stable and Unstable (Double Periodic Instability) Converter.

and unstable patterns (see Fig. 8.) . Once the gain for which instability occurred first had been found , it was recorded and a new case was measured. For the three different threshold sensor modes three different circuits were used, otherwise the techniques and the simulator circuits were the same.

We have conducted measurements for all three threshold sensor techniques, and for parameters of frequency :

$$2 \leq \nu \leq 20 ,$$

damping ratios :

$$\eta = .1 , .2 , .3 , .5 , .7 , \text{ and } 1. ;$$

and duty cycles of :

$$\delta = .1 , .2 , .3 , .4 , .5 , .6 , .7 , .8 , \\ \text{and } .9 .$$

Because of duality , there are 19 small signal stability curves in all. In the next section we shall show three of these curves as examples. All the other curves can be found in the technical report¹⁰.

V. EXAMPLES OF CURVES FOR CONVERTER DESIGN

We have described how small signal stability limits on the feedback gain ratio K_2/K_1 were determined for the two-loop serial boost Dc-to-Dc converter. In this section we shall discuss how these and other curves could help the designer in determining the right method for his converter design. These results are preliminary in the sense that the absolute stability question has to be solved before these design methods could be used for a practical converter circuit. Large signal oscillations might mask out the small signal stability limit in a practical converter. Furthermore, physical considerations will have to be investigated to close the circle for efficient design. Never the less , our results show the theoretically best possible design for our class of converters. Here we indicate that theoretically the best design is the one with the largest realizable feedback gain. The reason for this statement is that large feedback gain reduces the stringent requirement on the filter loss factor which arises from the requirement on good regulation. We are also convinced that large feedback gains improve the transient behaviour of the converter by reducing the settling time.

It is hard to tell at this time where the converter design will be started when the transient aspects and the physical aspects of the converter will be investigated. For now two of the four operating characteristics can be estimated : ripple and regulation. In fact, it is possible to solve for the stable , simply periodic mode of the converter for a given set of parameter values . The feedback gain does not appear in the equations. Once the periodic mode has been calculated, the ripple content of the output can also be calculated by evaluating the maximum and minimum voltages of the output , e_{out} . We have calculated the ripple content of the output voltage and on Figure 9. we show the summary of our calculations in the form of a graph. The ripple content is shown as a percentage of the output dc voltage and is a function of only two variables, frequency and

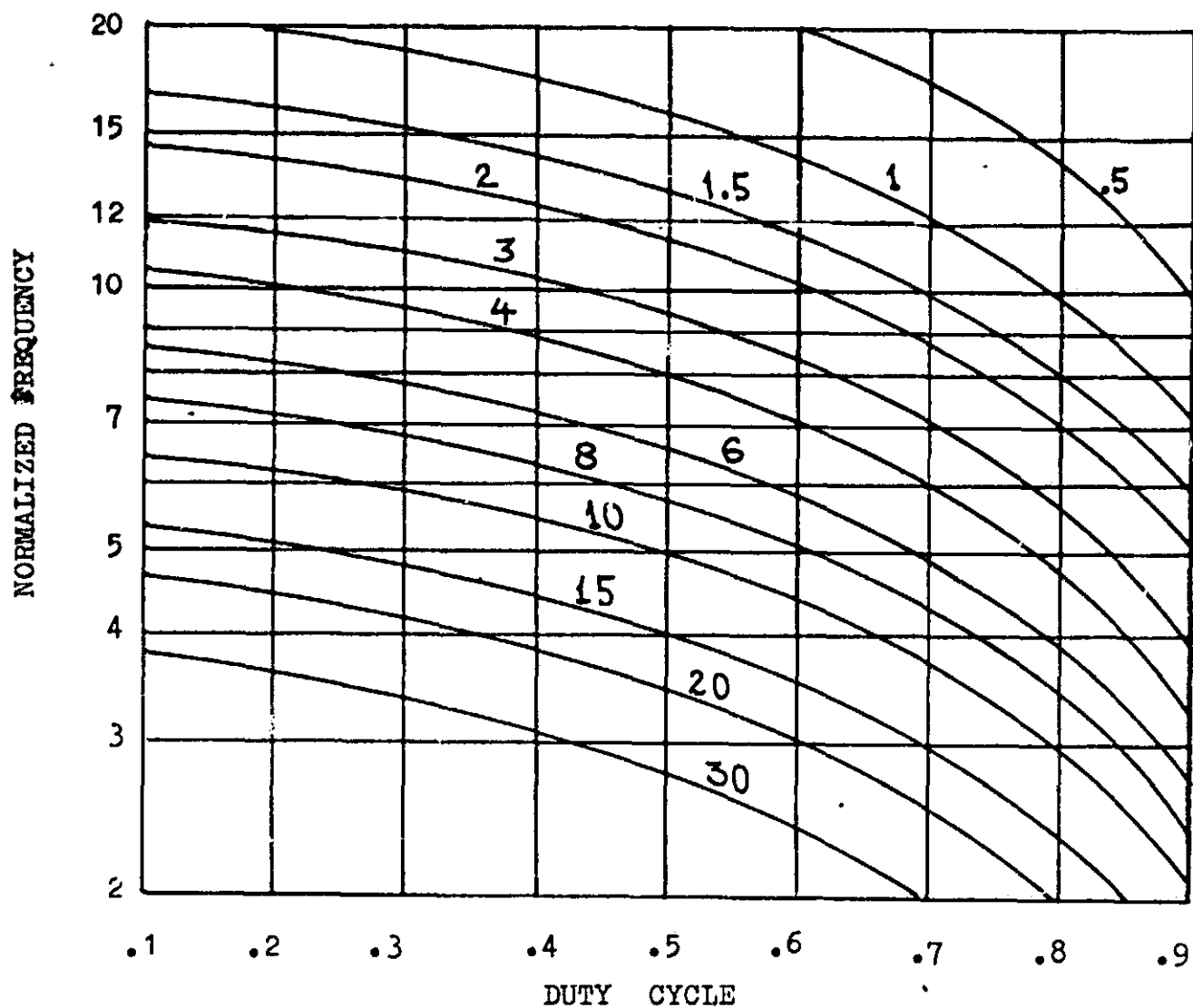


Figure 9. Percentage Ripple in e_{out} as function of Normalized Frequency and Duty Cycle.

duty cycle. These curves are in fact functions of the damping ratio, also, but they are very weak functions of the damping ratio, therefore their functional dependance on the damping ratio is not shown. The damping ratio effects the curves only for very large ripple contents, which are not practical, anyway.

We have shown that the duty cycle can be calculated from physical considerations; therefore Figure 9. can be thought of as the graph which places a restriction on the normalized frequency if a required minimum ripple content is specified. In many applications the switching frequency has an upper limit due to the power switches used and the allowable power loss while switching; therefore, the normalized frequency value and the switching frequency determine the resonant frequency of the filter.

The following three curves, Figs 10 - 12. show the small signal stability curves for the three principal methods of threshold sensors. All three curves are shown are for duty cycle value of .3. The parameter on the different curves is the damping ratio. The stability curves exhibit discontinuities, or discontinuous derivatives. Usually at these discontinuities the instability mechanisms change, from doubly periodic mode to run-away mode, for example. For example, for the free running case (see Fig. 10) at normalized frequency value of 7, the feedback gain value that is the limit on stability is 10 for damping ratio of .5 and is approximately 20 for damping ratio of .7. For damping ratio of .5 the mode of instability changes at normalized frequency 5.8 where the instability mechanism changes from doubly periodic mode to the run-away mode. For the constant T_{on} case, for damping ratio of .5 or lower and frequencies lower than 4.5 we have only one curve. While, for the same set of curves for frequency of 10 there is a large difference for the curves with damping ratios .2, .3, and .5. This shows again that more than one modes of instability are involved.

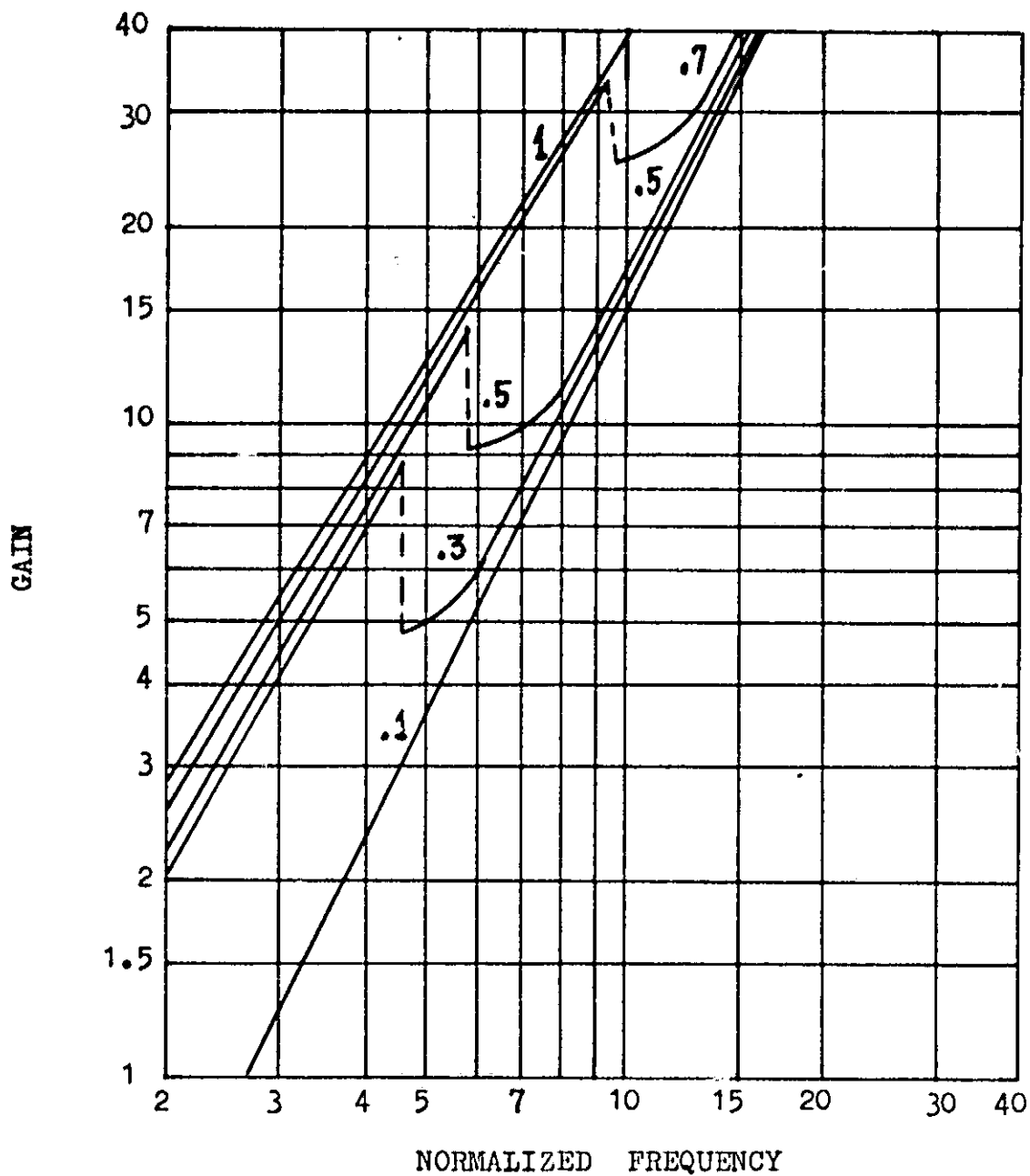


Figure 10. Stability Limit on the Feedback Gain for the Free-Running Threshold Sensor. Duty Cycle = .3
The parameter is the damping ratio.

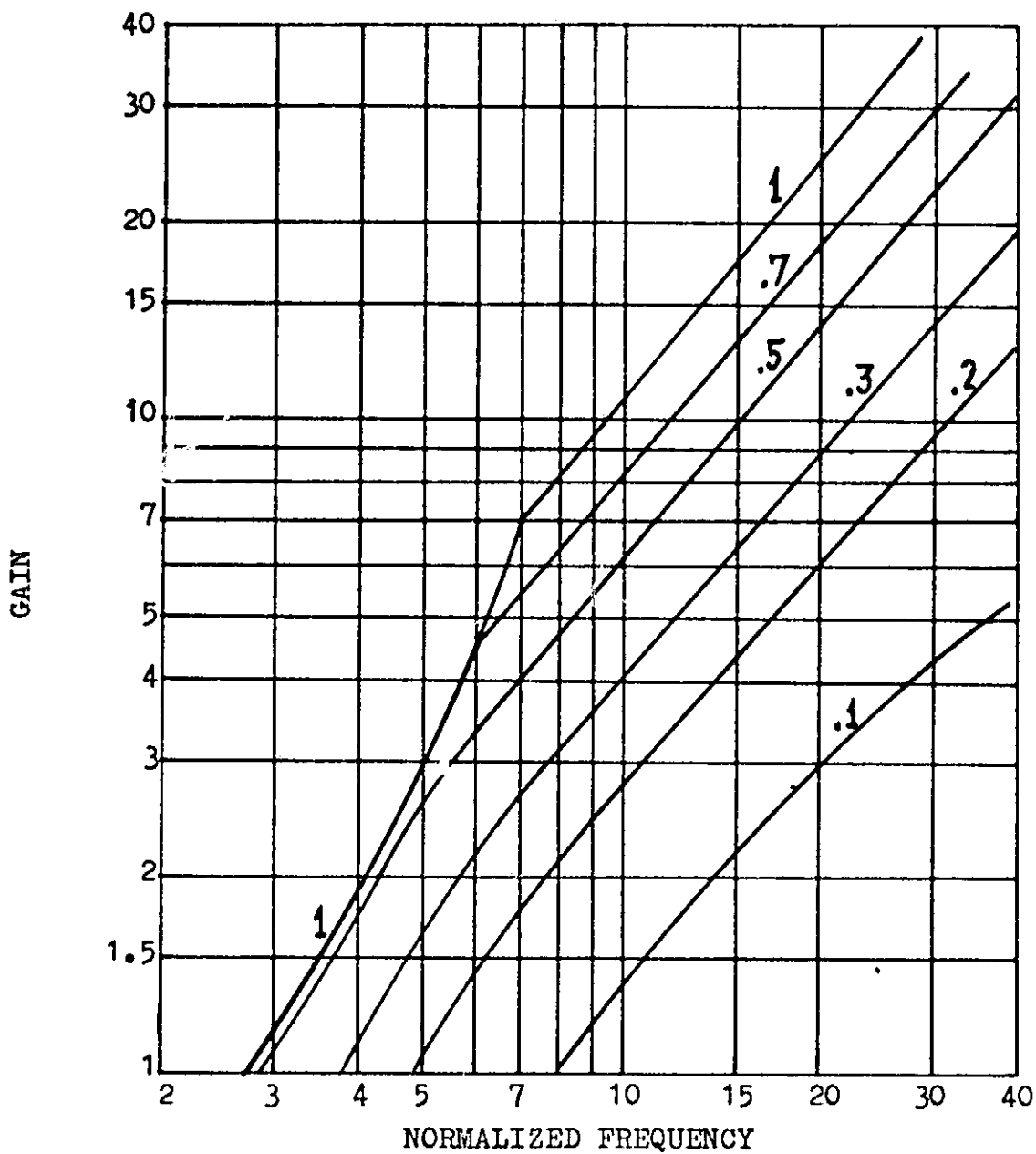


Figure 11. Stability Limit on the Feedback Gain for the Synchronized Threshold Sensor. Duty Cycle = .3
The parameter is the damping ratio.

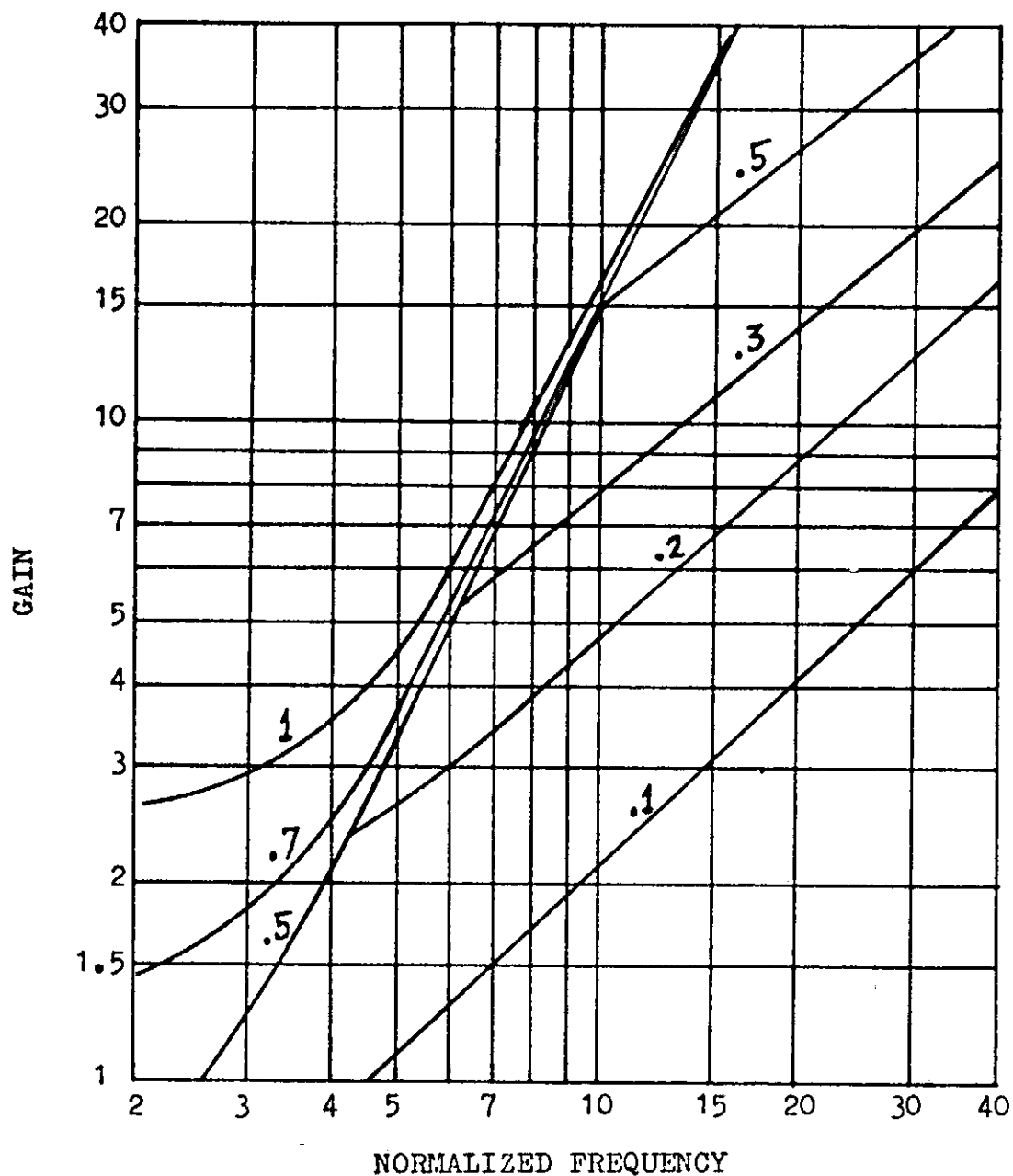


Figure 12. Stability Limit on the Feedback Gain for the Constant ON-time Threshold Sensor. Duty Cycle = .3
The parameter is the damping ratio.

The three curves shown are actually include six cases, because the curves are the same for the dual methods and with the substitution of $1 - \delta$ in the place of δ . Therefore, the free running case curves are also used for duty cycle of $1 - .3 = .7$, the synchronized curves are correct for the dual synchronized case and with duty cycle of $.7$, and the constant T_{on} curve is used for the constant T_{off} threshold sensor and with duty cycle of $.7$. Comparison of these three curves indicate that in general, the free-running case has the highest feedback gain limit while the synchronized case seems to have the lowest.

From the physical voltages e_{on} , e_{off} , and e_{ref} , the range of usable duty cycles are determined, (See Table I.). From limits on the ripple content the normalized frequency value is deduced. From the loading factor of the filter the damping ratios might be calculated. Then the stability curves place limitations on the feedback gain. Finally, the feedback gain determines the relationship between the regulation and the filter loss factor :

$$\text{Regulation} = \frac{1 - r}{1 + r \cdot K}$$

which is Equation (25) repeated here. These considerations might be considered as a first step in the converter design process.

VI. CONCLUSIONS

We have set out a limited aim in this article and we have succeeded reaching it. We have selected a narrow class of Dc-to-Dc converters and found useful tools of analysis for it. We have generated data that can be used to calculate the theoretically best possible converter configuration of this class as far as the small signal stability of the converter is concerned. And we have hope that the large signal stability problem will lend itself to a practical solution. Finally , still keeping in this same narrow class of converters, the analysis of the physical characteristics of these converters might give us a plausible design method in the future. It might also be necessary to consider more complicated converter schemes such as the serial buck , or the buck-boost circuit configurations. At this time it is not obvious that these more complicated circuits offer any advantages to the converter designer.

LIST OF REFERENCES

1. Andeen, R.E. "Analysis of Pulse Duration Sampled-Data Systems with Linear Elements," IRE Trans. on Auto Control, Vol. AC-5 , No. 4, Sept., 1960, pp 306-313
2. Jury, E.I., Nishimura, T., "On the Periodic Modes of Oscillation in Pulse-Width-Modulated Feedback Systems," Trans. of ASME Jour. of Basic Eng., Vol. 84, Ser. D, No. 1, March, 1962, pp. 71-84
3. Jury, E.I., Nishimura, T., "Stability Study of PWM Feedback Systems," Trans of ASME, Jour. of Basic Eng., Vol. 86, ser. D, No. 1, March, 1964, pp 80-86
4. Wolaver, D.H. , "Fundamental Study of DC to DC Conversion Systems," ESL-R-376 , Report, Elec.Sys.Labs., M.I.T., Cambridge, Mass. , Feb, 1969.
5. Blankenship, G.L., "Stability Criteria for Pulse-Width-Modulated Feedback Systems Using Loop Gain Conditions," Master Thesis, M.I.T., Cambridge, Mass. June, 1969
6. Schwarz, F.C., "Power Processing," NASA SP-244, 1971
7. Lalli, V.R., Schoenfeld, A.D. , "Asdtic Duty-Cycle Control for Power Converters," NASA TM X-68066, May, 1972
8. Schoenfeld, A.D., Yu, Y. , "The Application of the Analog Signal to Discrete Time Interval Converter to the Signal Conditioner Power Supplies," NASA CR-120906, August, 1973
9. Schwarz, F.C., "Engineering Information on an Analog Signal to Discrete Time Interval Converter (ASDTIC)", NASA CR-134544 June, 1974
10. A technical report on this research is under preparation.

PART II.

Detailed Results.

APPENDIX A. FEEDBACK GAIN LIMITS FOR STABILITY

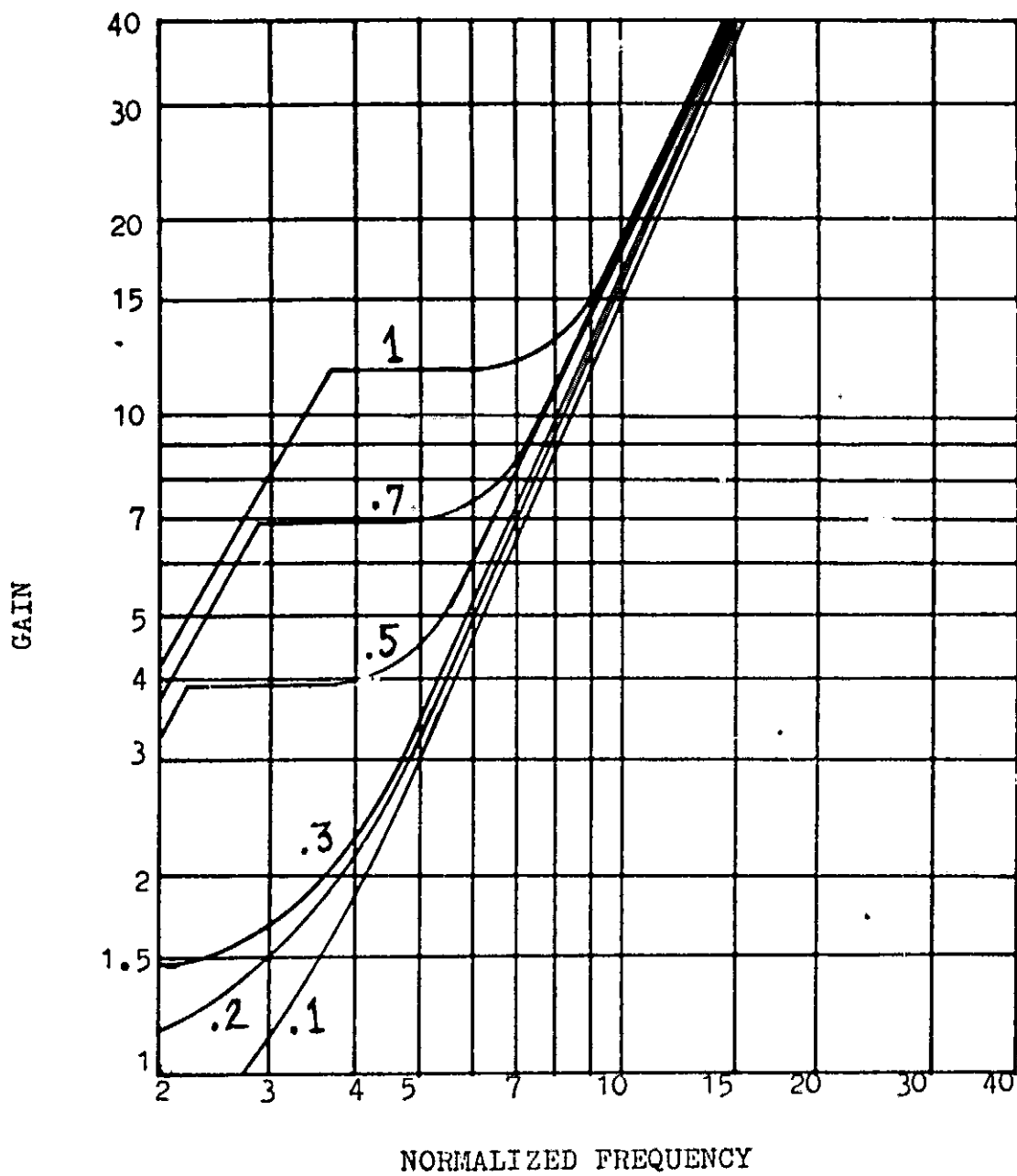
In this appendix we summarize the analog computer studies described in the preceeding paper. The limits on the feedback gain for small signal stability are shown on nineteen diagrams. The first five are for the free-running case , the following five curves are for the synchronized case , and finally, the last nine curves are for the constant T_{on} case. There are only five curves for the free-running case because when ϕ , the duty cycle is replaced by $1 - \phi$, the same curve can be used. There are only five curves for the synchronized case, because the synchronized case is not stable for duty cycles larger than .5 . However , the curves for the synchronized case and for the constant T_{on} case can be used for their dual cases (as described in the preceeding paper) by substituting $1 - \phi$ in place of ϕ .

In all the following curves the parameter is the damping ratio , η , which is assigned the following values :

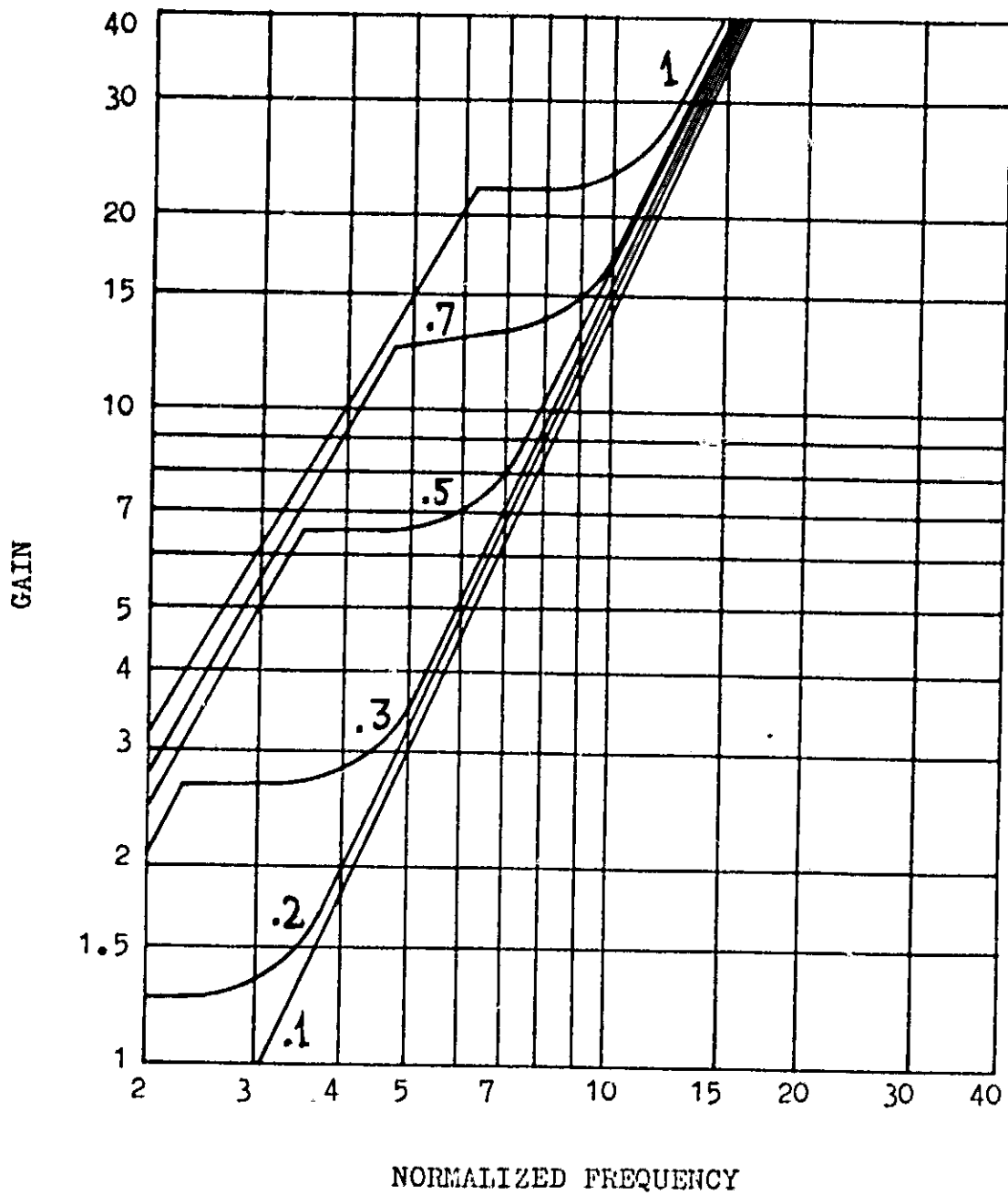
$$\eta = .1 , .2 , .3 , .5 , .7 , 1 .$$

Hence, for each diagram there will be a family of six curves. The horizontal axis shows values of the frequency ratio , ν , and the vertical axis gives the values of the feedback gain.

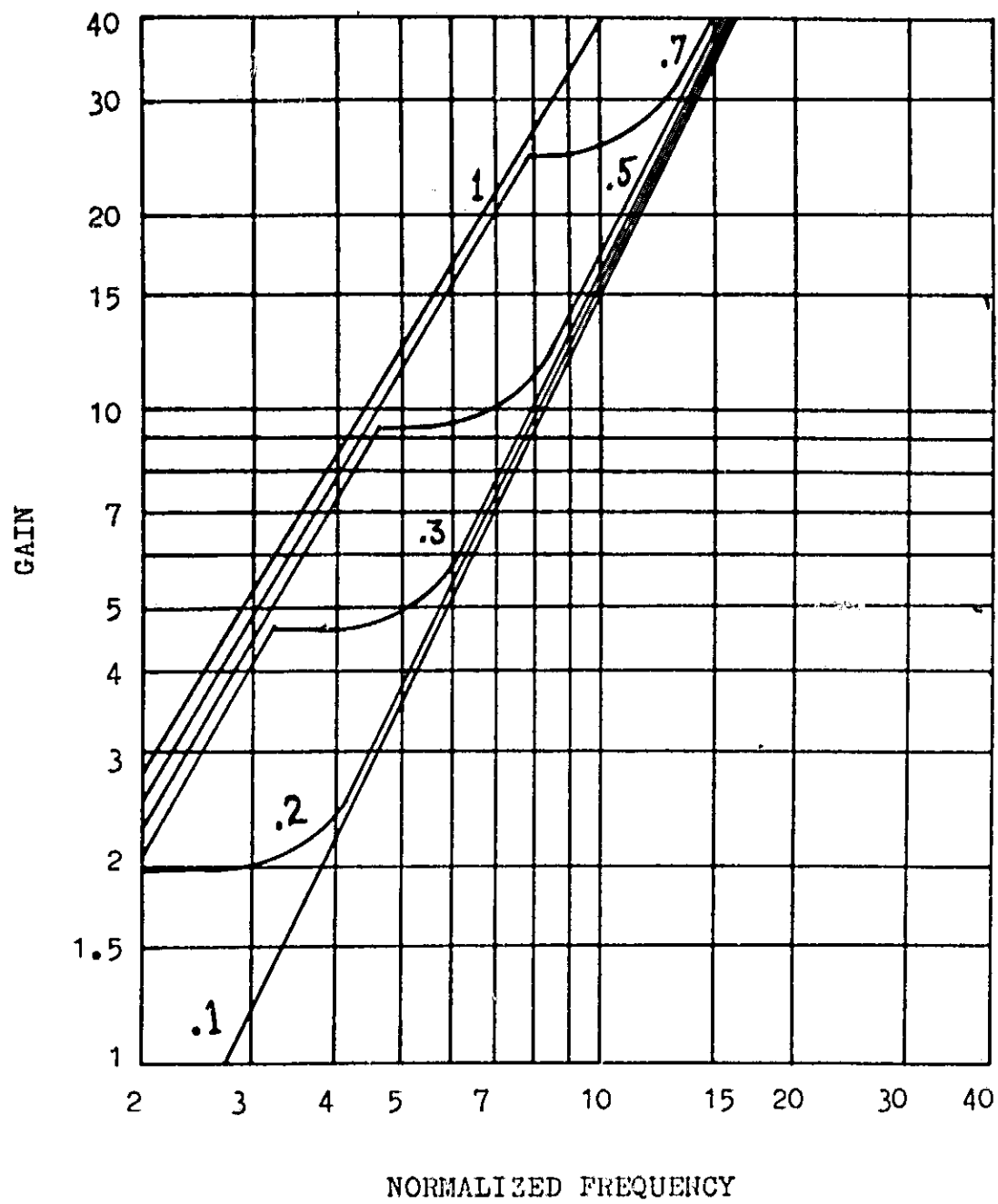
A.1. STABILITY LIMIT CURVES FOR THE FREE-RUNNING CASE



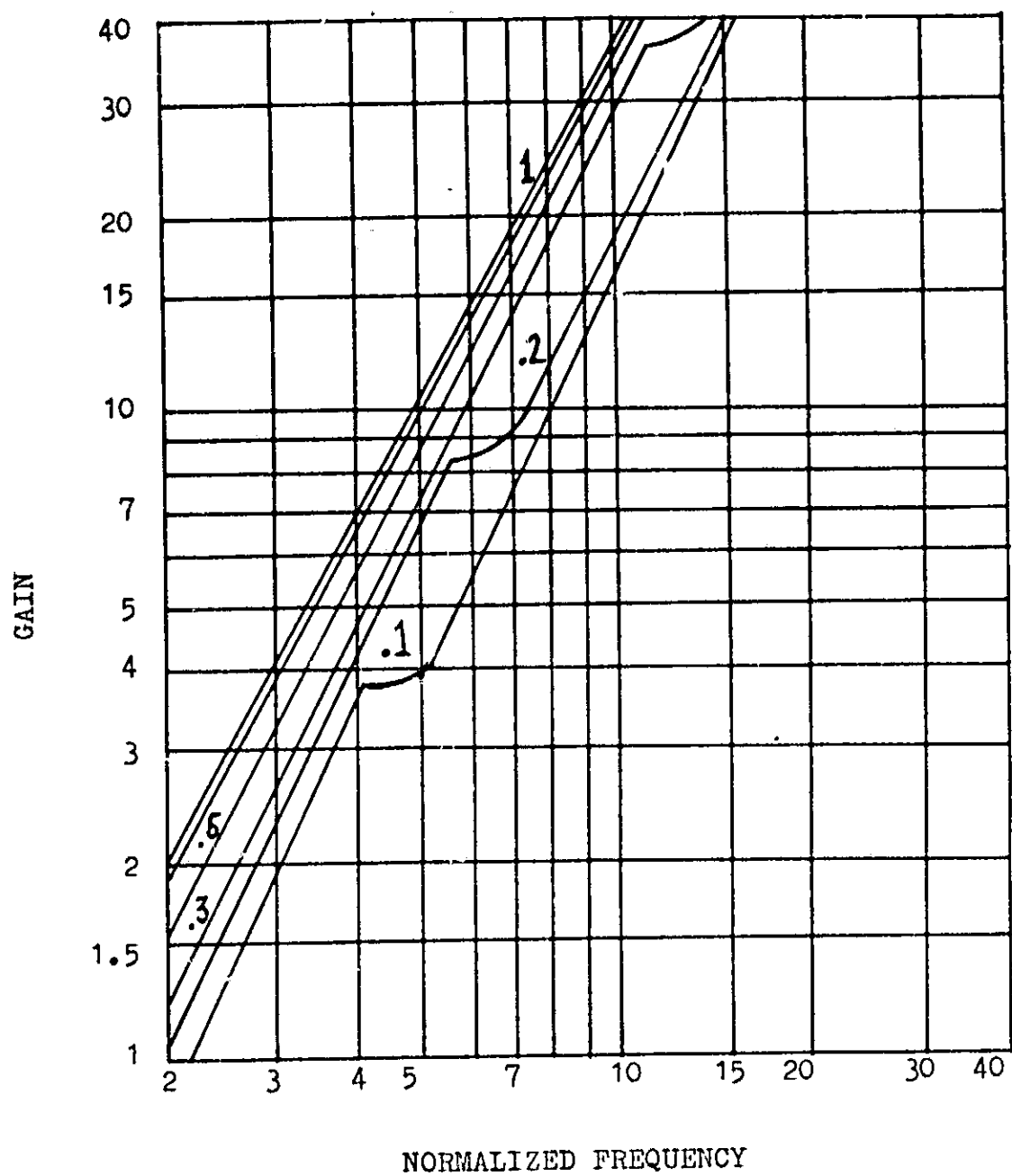
Duty Cycle = .1 or .9



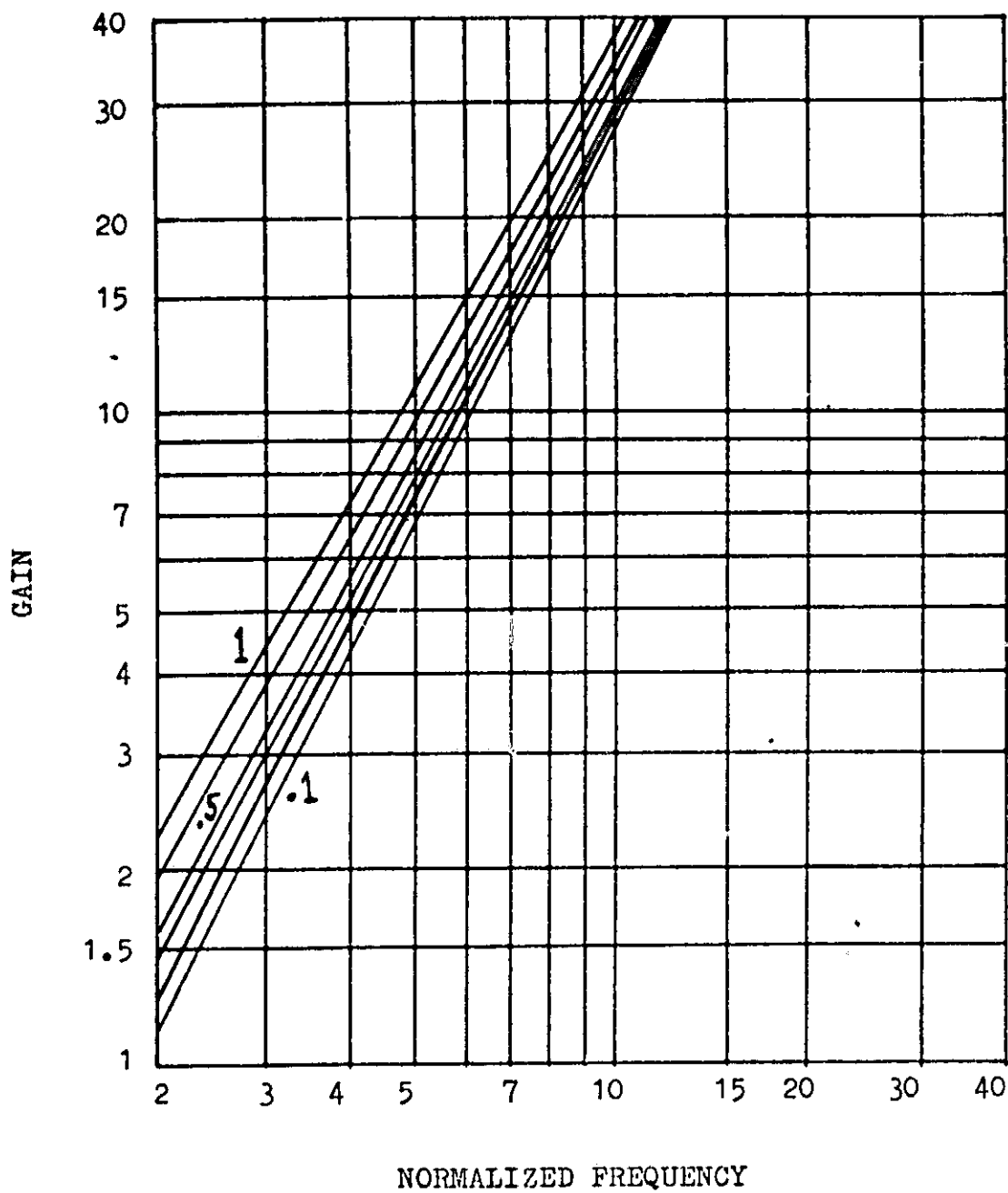
Duty Cycle = .2 or .8



Duty Cycle = .3 or .7

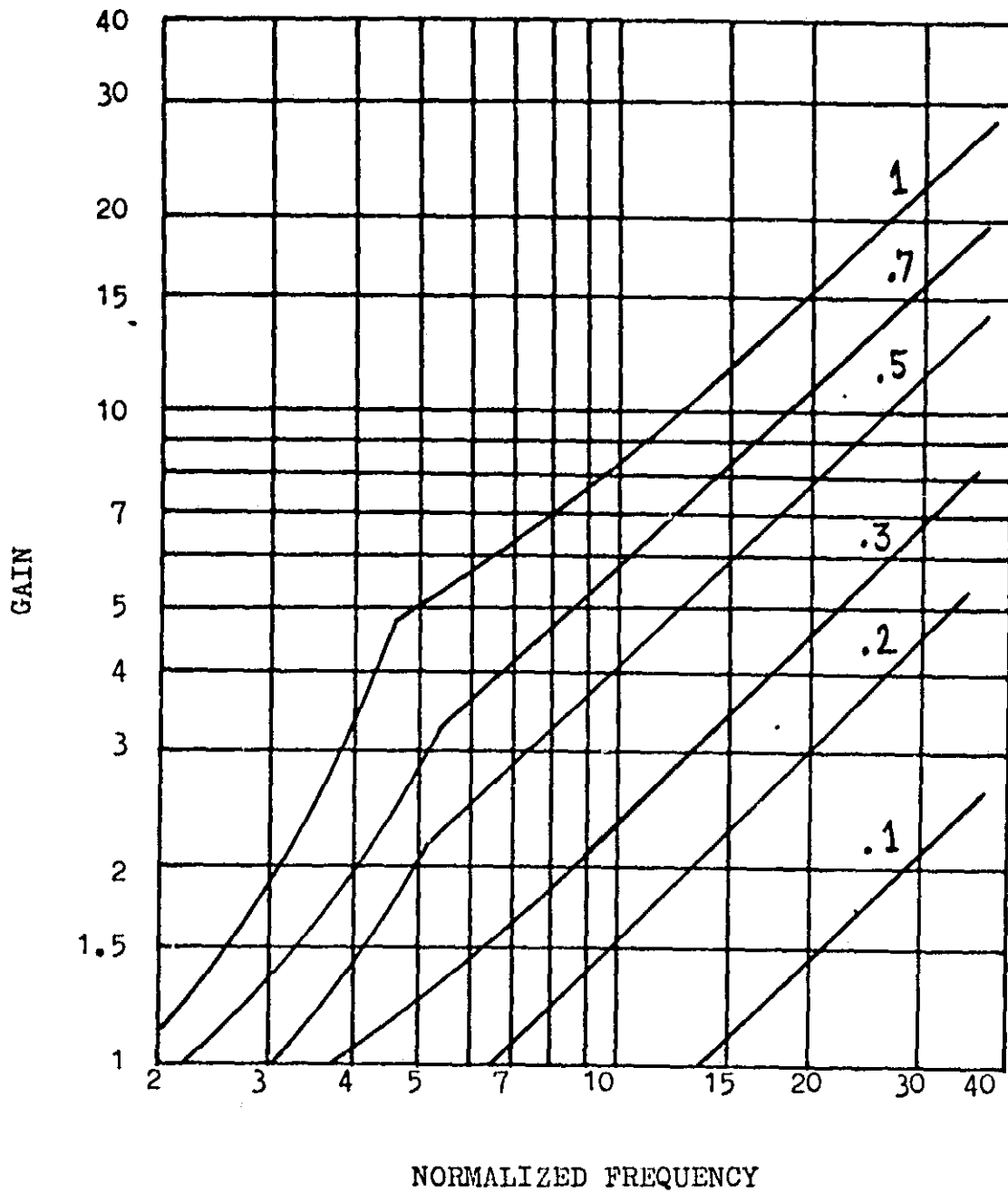


Duty Cycle = .4 or .6

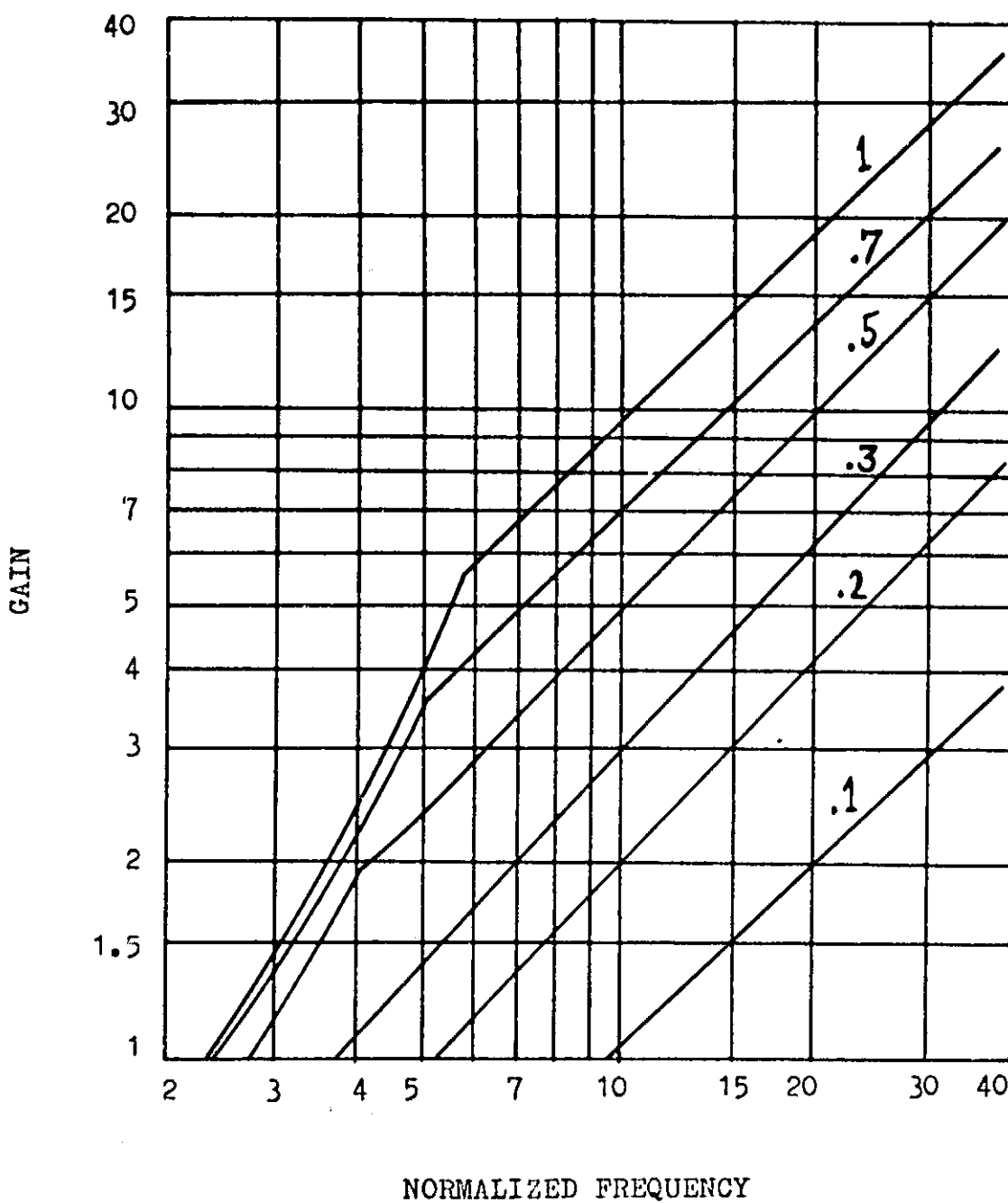


Duty Cycle = .5

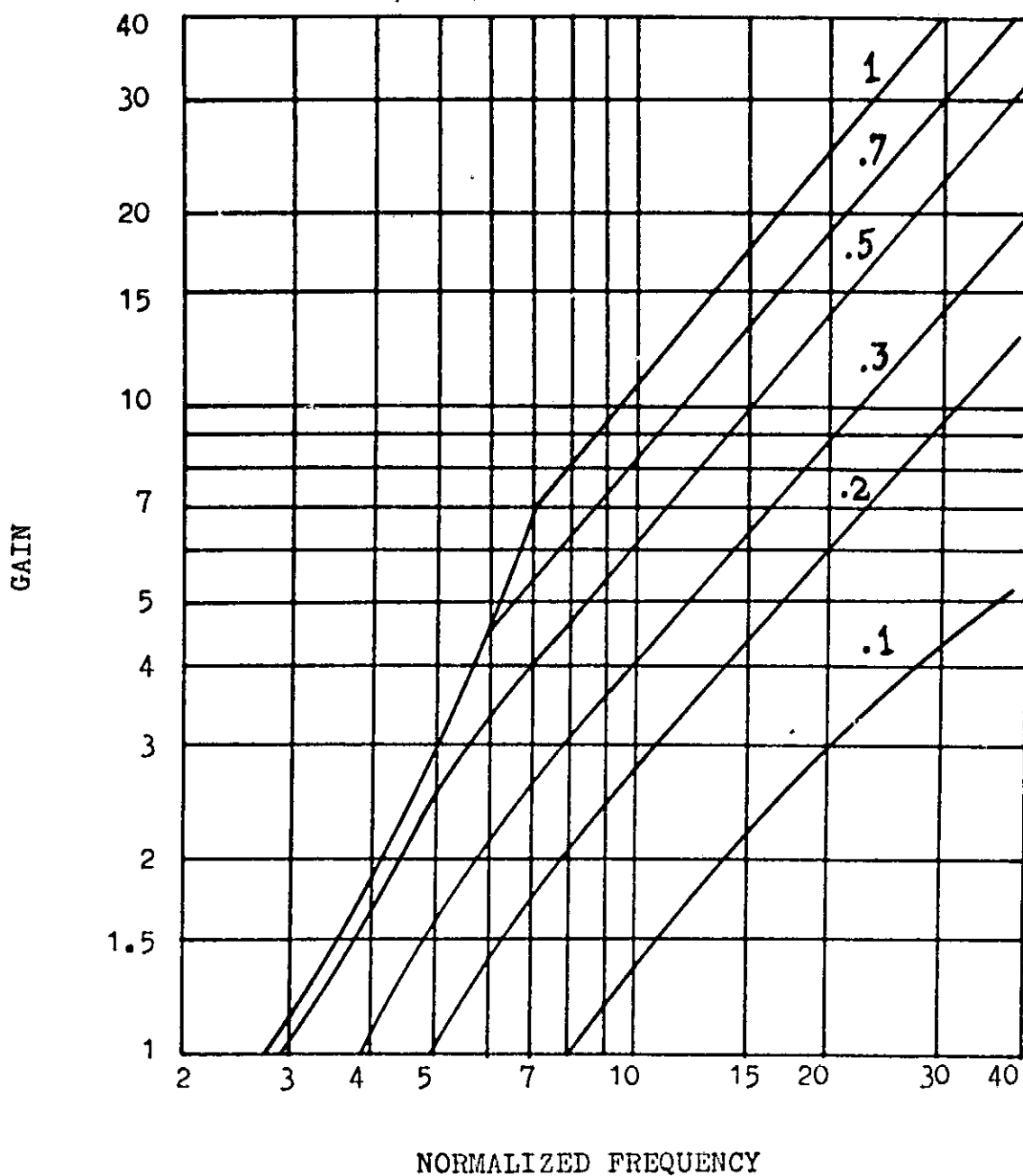
A.2. STABILITY LIMIT CURVES FOR THE SYNCHRONIZED CASE



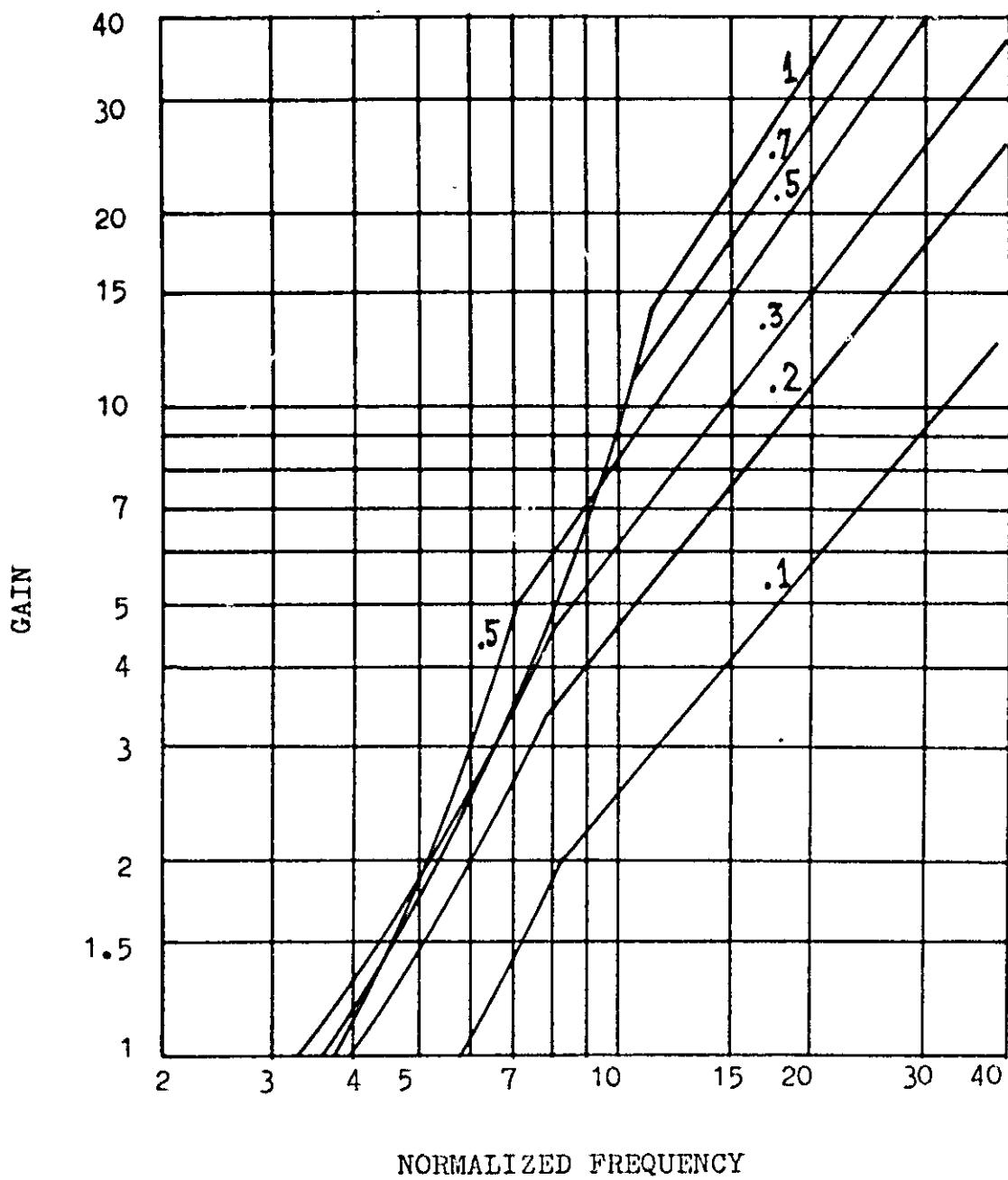
Duty Cycle = .1 (Dual Case = .9)



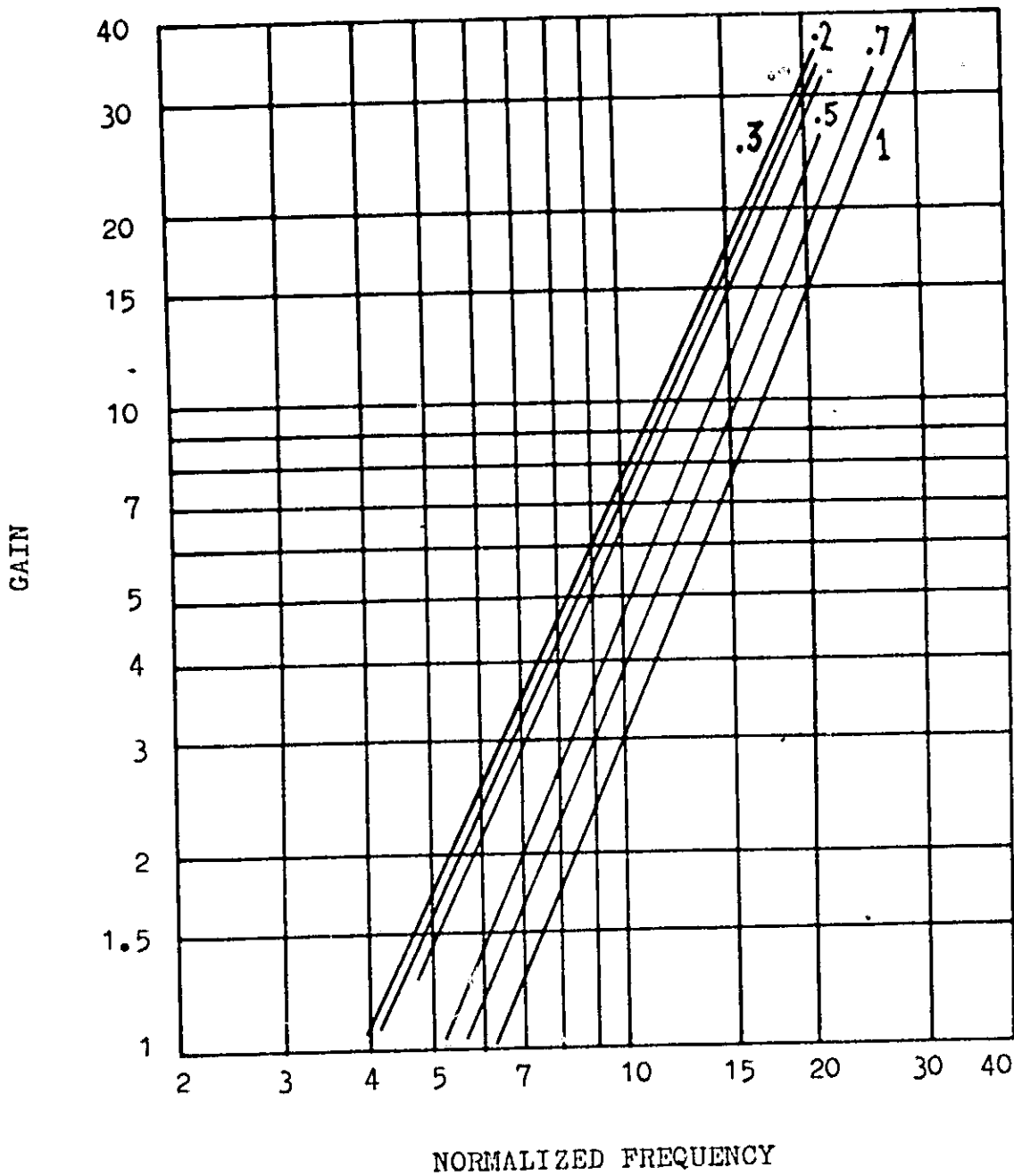
Duty Cycle = .2 (Dual Case = .8)



Duty Cycle = .3 (Dual Case = .7)

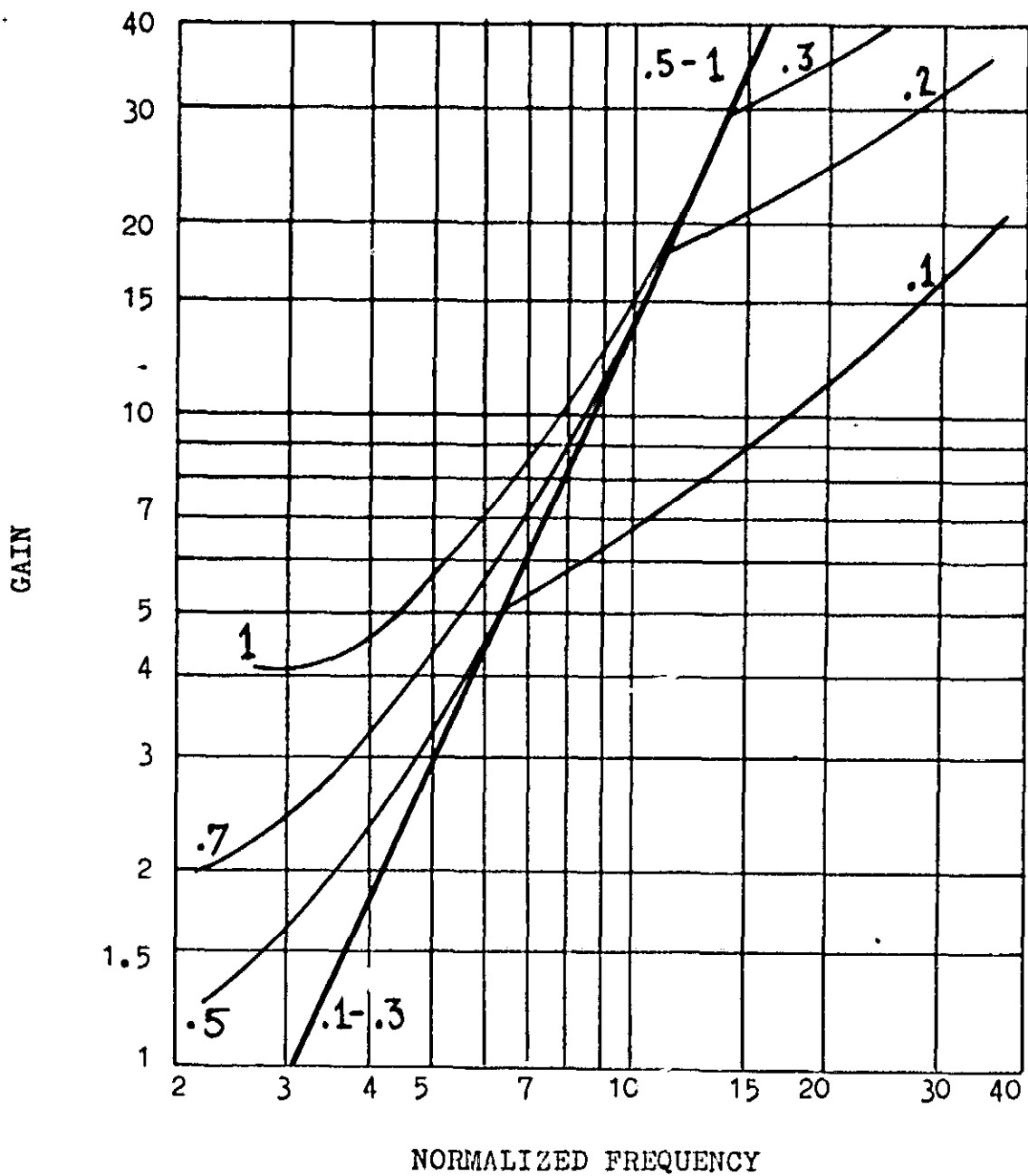


Duty Cycle = .4 (Dual Case = .6)

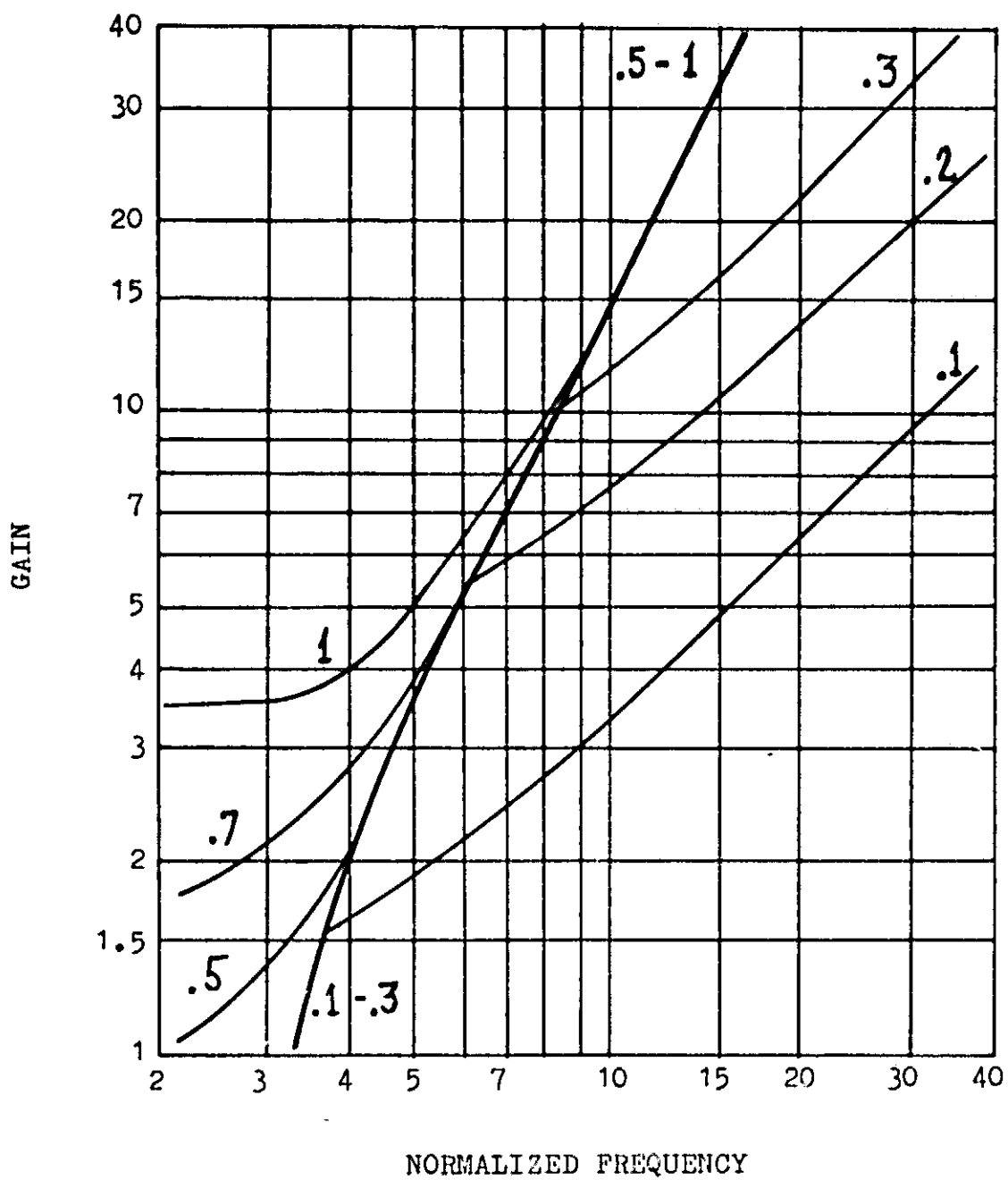


Duty Cycle = .48 (Dual Case = .52)

A.3. STABILITY LIMIT CURVES FOR THE CONSTANT T_{on} CASE

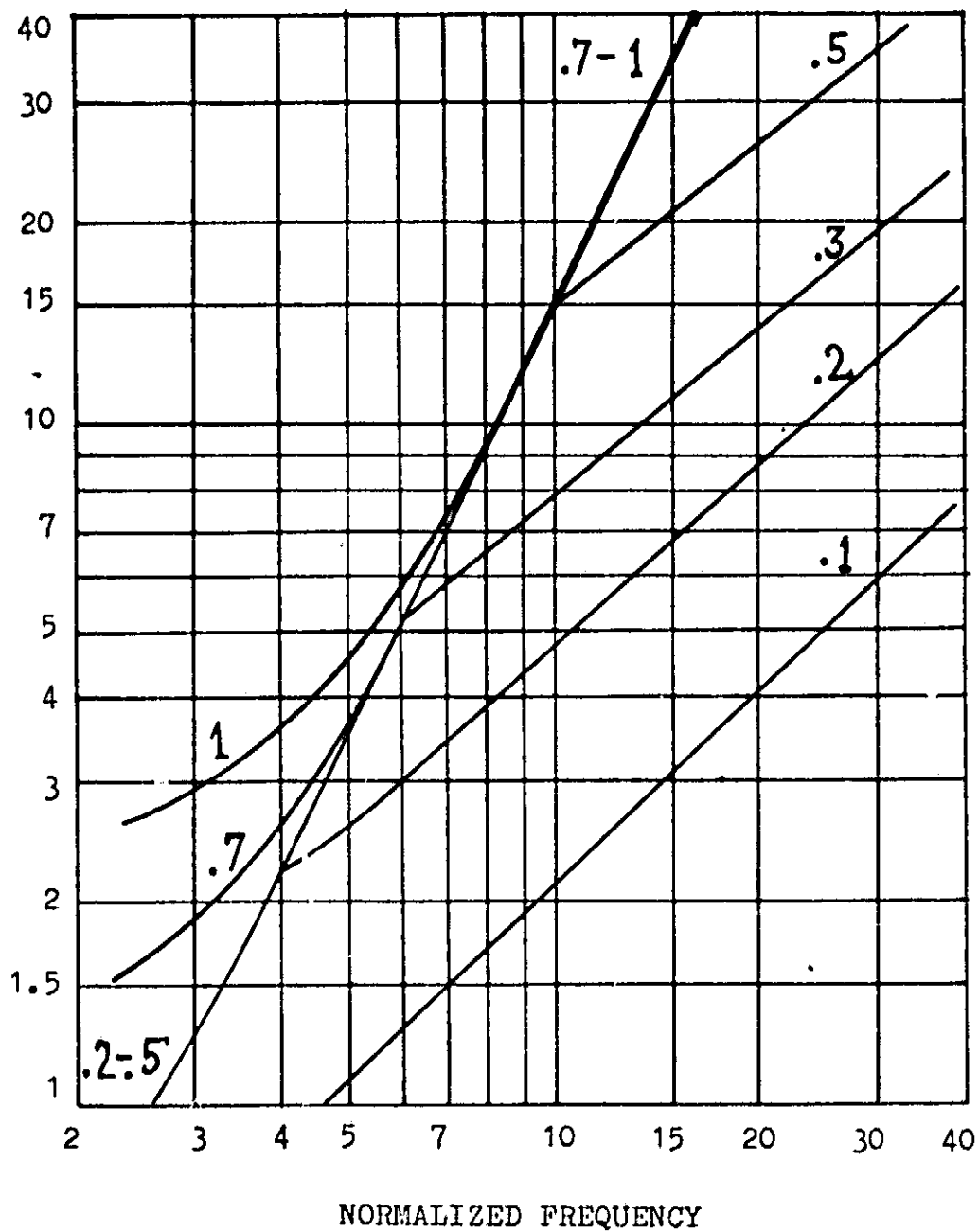


Duty Cycle = .1 (Dual Case = .9)

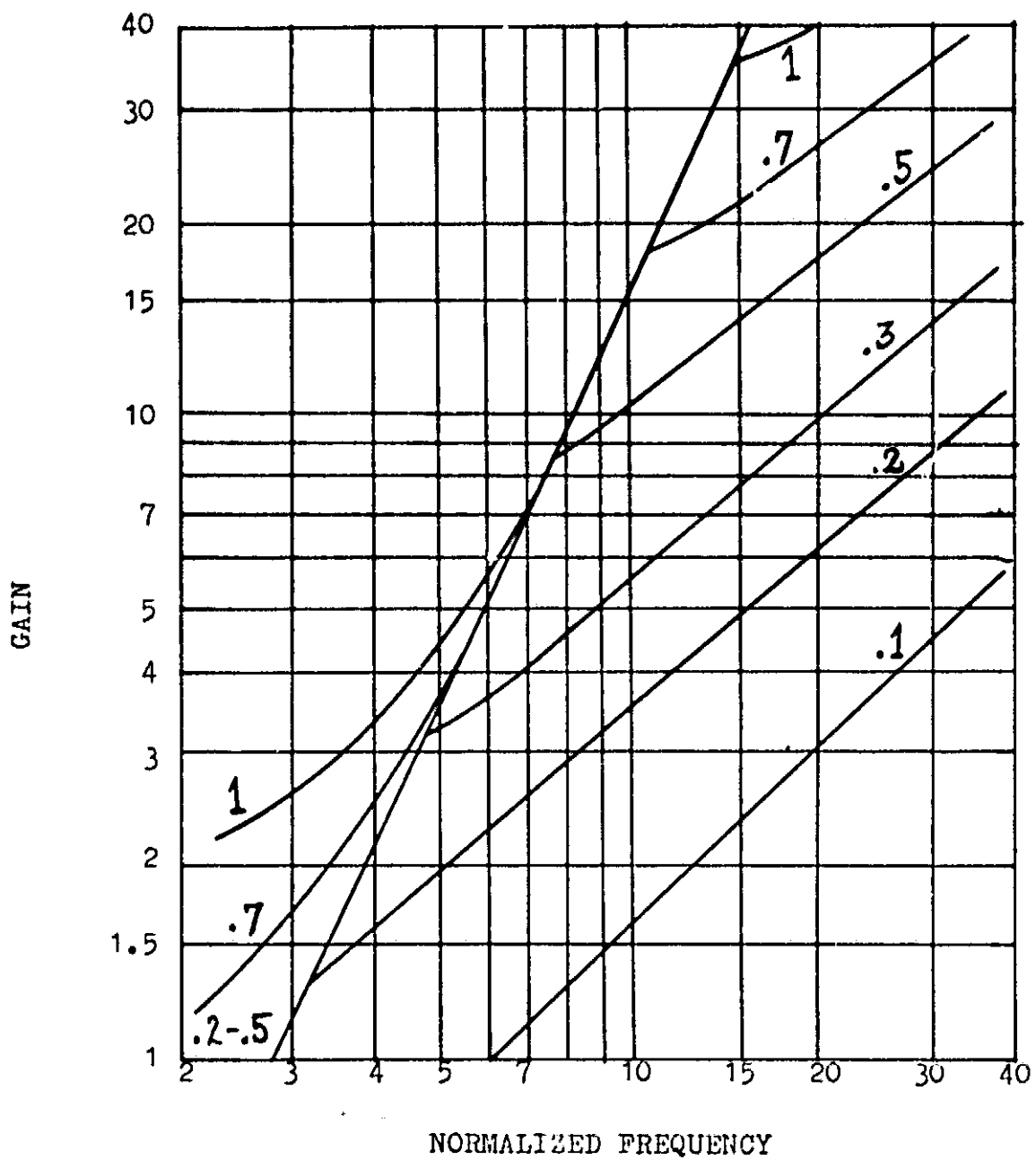


Duty Cycle = .2 (Dual Case = .8)

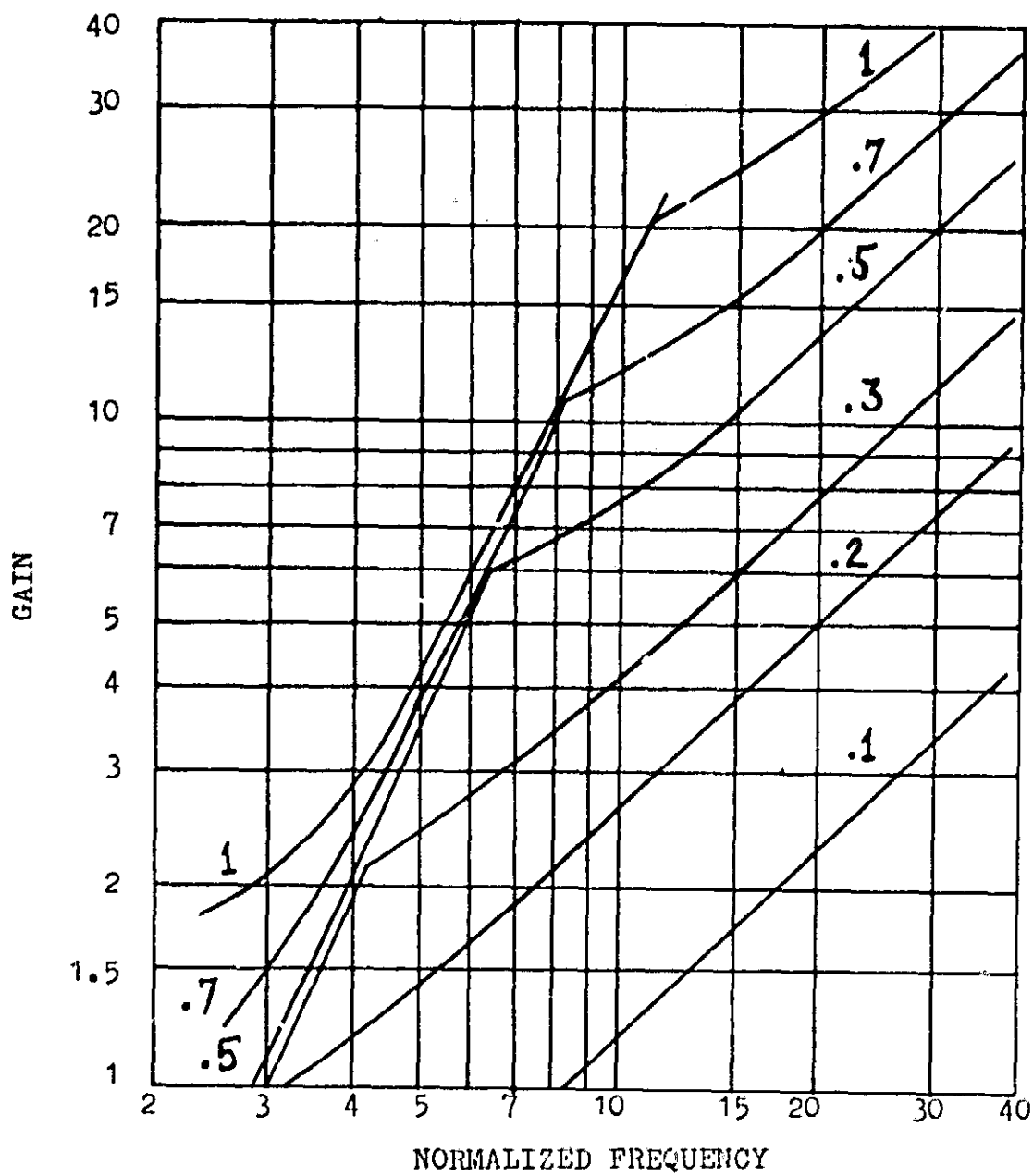
GAIN



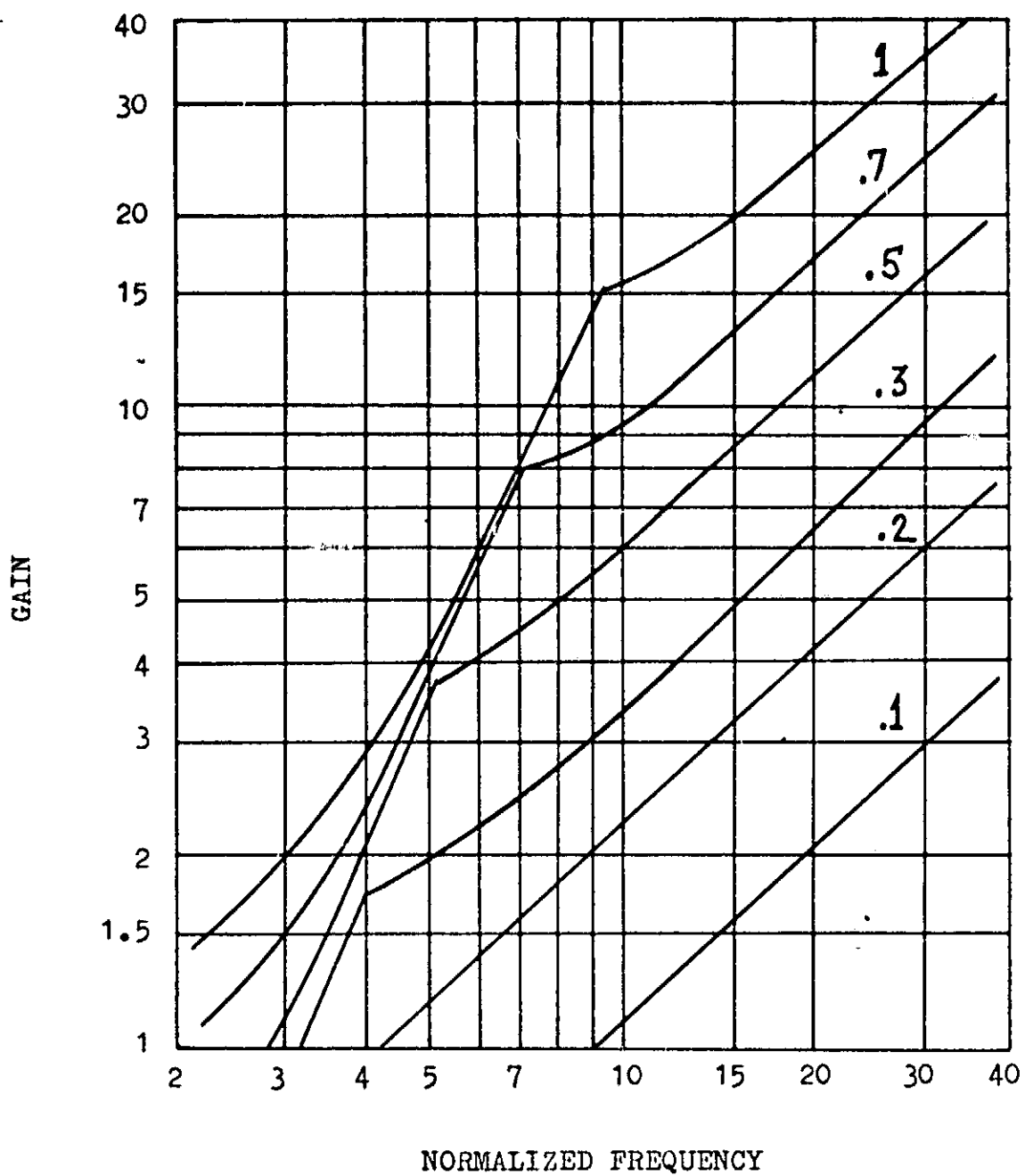
Duty Cycle = .3 (Dual Case = .7)



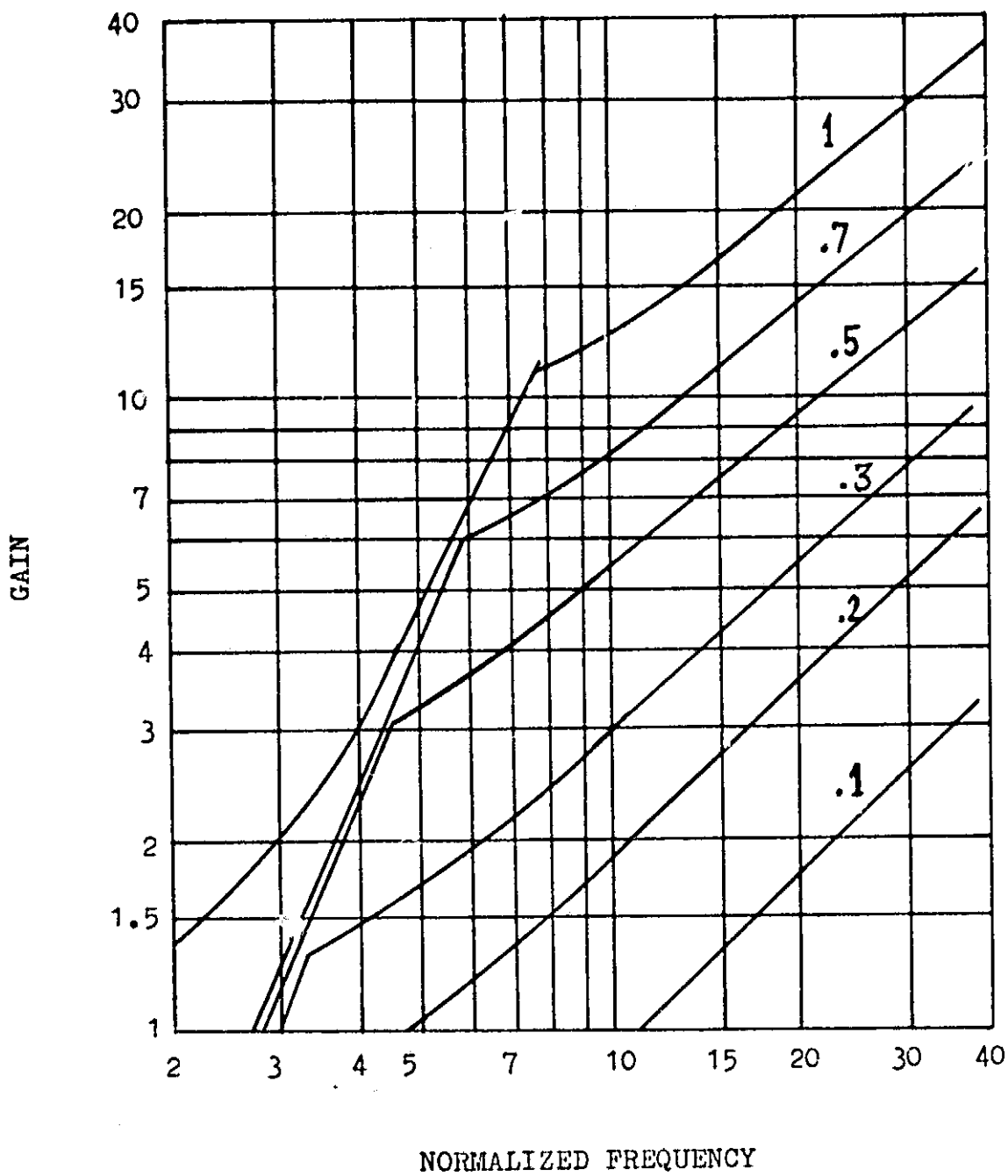
Duty Cycle = .4 (Dual Case = .6)



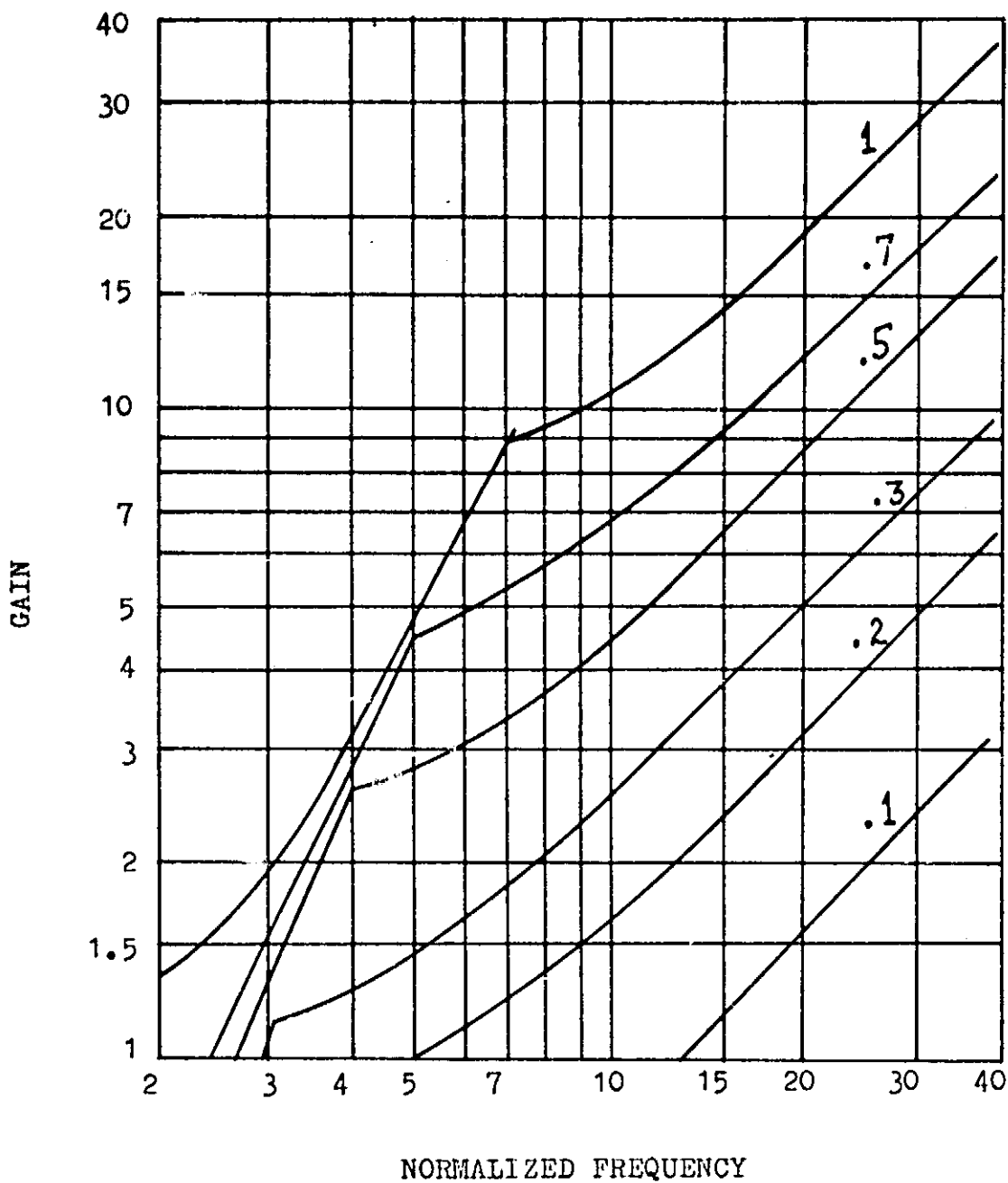
Duty Cycle = .5 (Dual Case = .5)



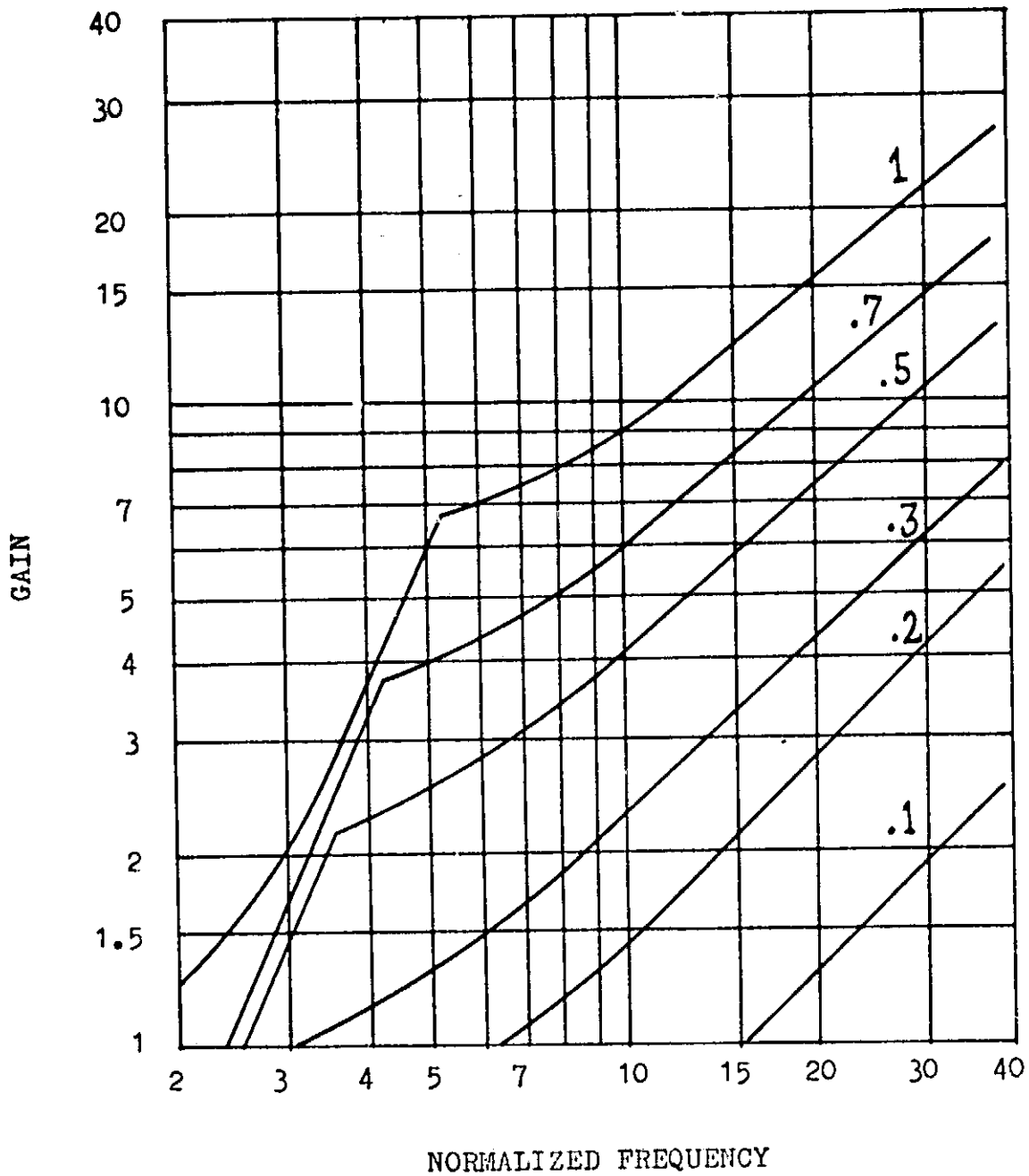
Duty Cycle = .6 (Dual Case = .4)



Duty Cycle = .7 (Dual Case = .3)



Duty Cycle = .8 (Dual Case = .2)



Duty Cycle = .9 (Dual Case = .1)

APPENDIX B. ANALOG COMPUTER CIRCUITS

In this appendix we present the analog computer circuits used for our simulation studies. The precision ten-turn potentiometers are designated as P_1 to P_6 . The operational amplifiers were precision chopper stabilized amplifiers. The resistors were precision temperature compensated resistors. Drifting of the characteristics were negligible.

Most circuits which follow are self explanatory. The threshold sensor/switch circuitry were used for all three cases in the following manner. For the free running case only input # 1. was used for v_{cont} . (See paper for details). For the synchronized case the gain in the integrator was the lowest possible (very low frequency) and the second input in the threshold sensor/switch was connected to a pulse generator which synchronized the operation of the switch. For the constant T_{on} case the second input was connected to a one-shot multivibrator , whose T_{on} time was adjusted by another external potentiometer.

The frequency of the regulator was measured with a counter. The other parameters were set by the precision potentiometers. The potentiometers were calibrated using a digital computer through an analog-to-digital converter.

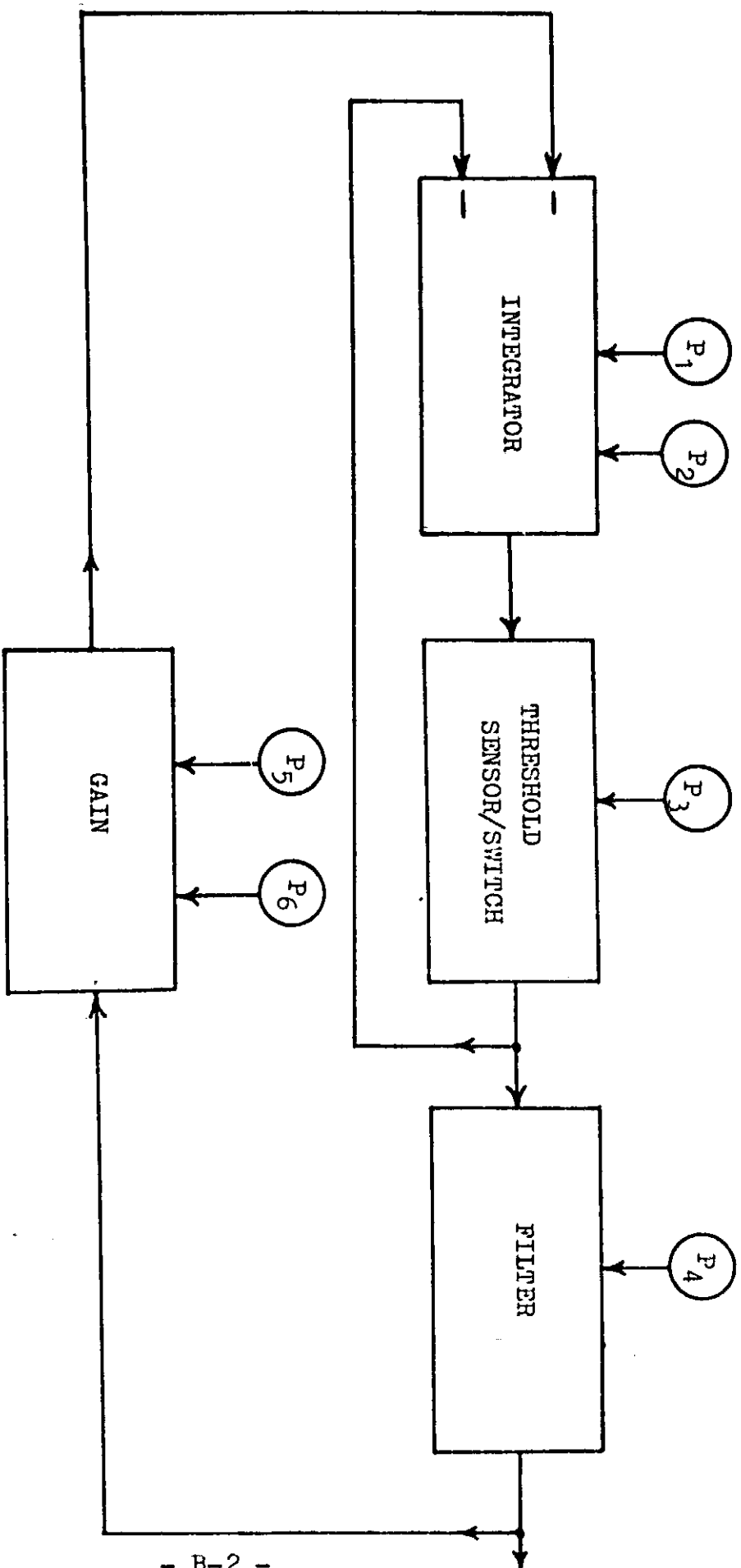
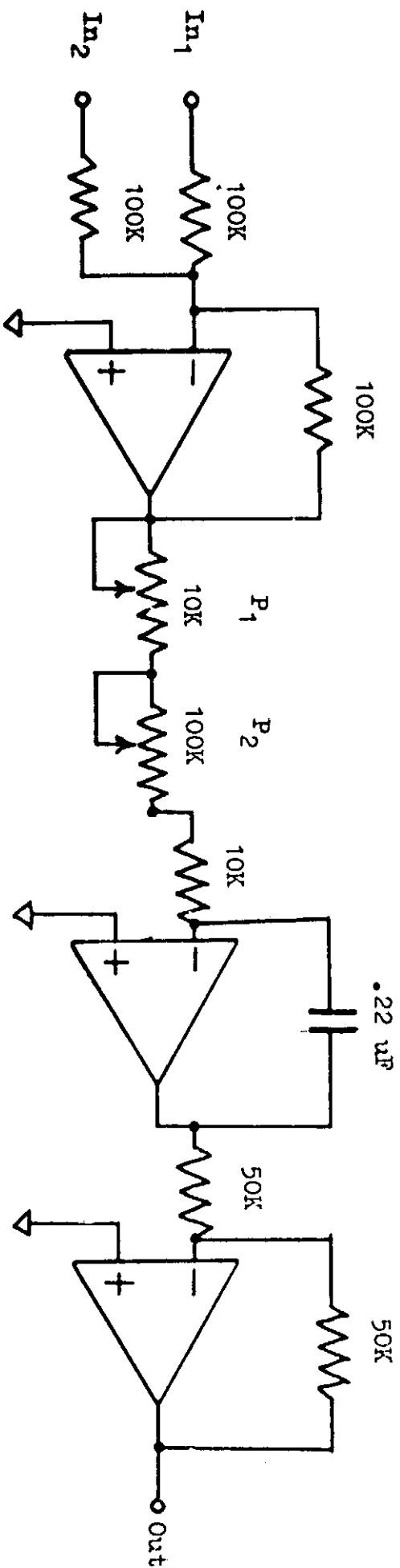


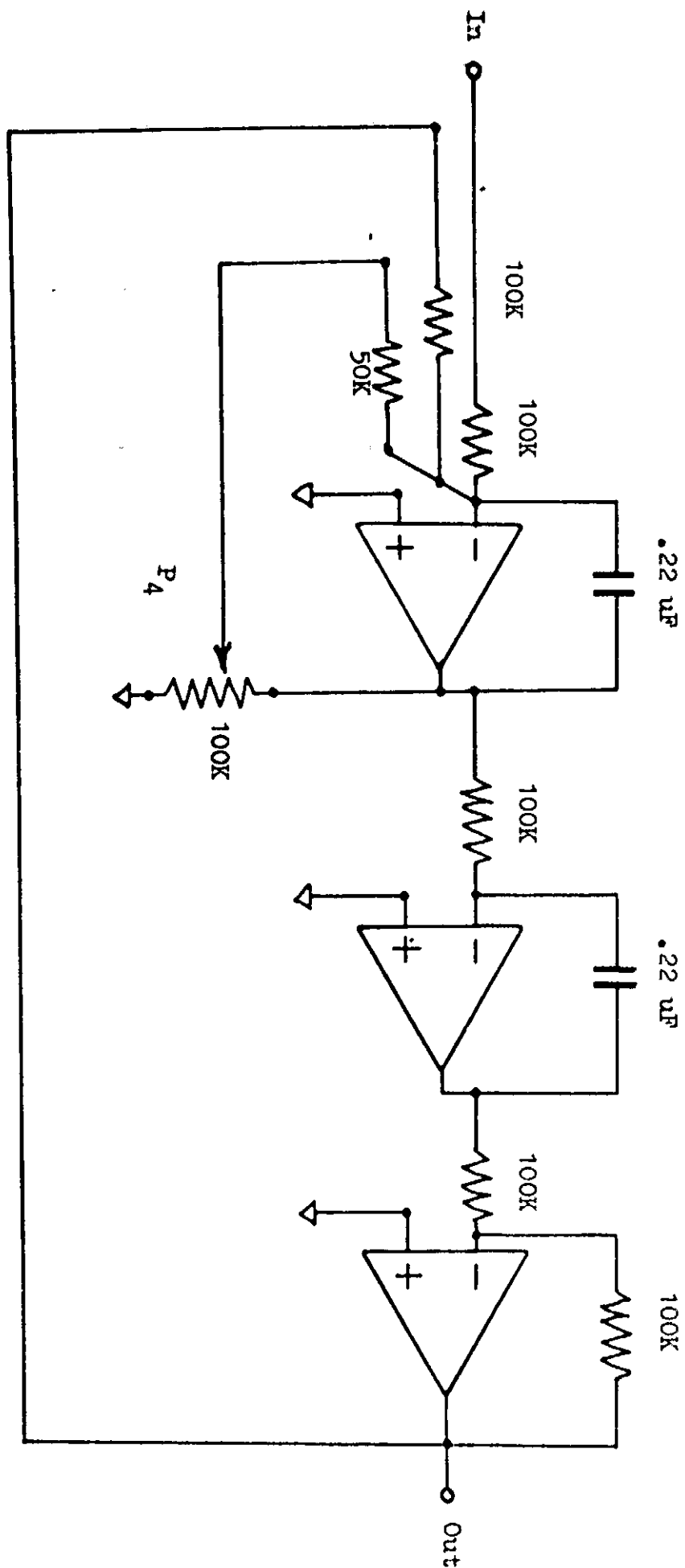
Figure B.1. Overall Block Diagram



Both P_1 and P_2 adjust the frequency of the regulator. P_1 is fine, P_2 is coarse adjustments.

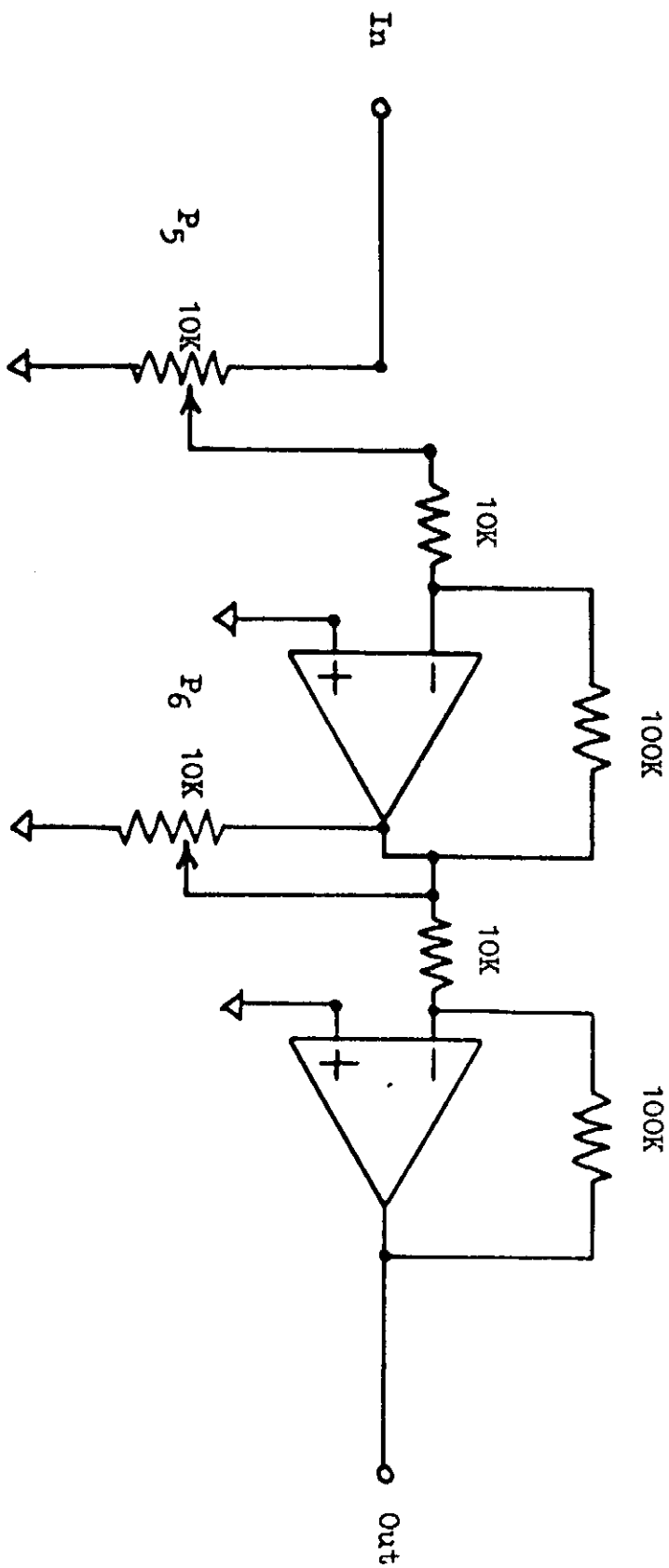
Figure B.2.

The Integrator Circuitry



P_4 adjusts the damping ratio from 0 to 1.

Figure B.4. Low Pass Filter Circuitry



Both P_5 and P_6 adjust the feedback gain. The total gain is the product of the two gains which ranges from 0 to 100 .

Figure B.5. The Feedback Gain Circuitry

APPENDIX C.

DERIVATION OF THE RIPPLE EQUATION

The ripple magnitude of the output voltage can be calculated exactly. The derivation is given on the following pages. The actual calculation was done on a digital computer and the combined results shown on the ripple diagram included in the paper. The parameters are :

Normalized frequency , ν

Duty Cycle , ρ

and Damping ratio , η

The normalized times T (period) , T_{on} and T_{off} can be directly calculated from the normalized frequency :

$$T = 2\pi / \nu$$

$$T_{on} = \rho \cdot T$$

$$T_{off} = (1-\rho) \cdot T$$

The damping ratio , η , determines the two poles for the second order low pass filter p_1 , and p_2 as :

$$p_1 = -\eta + \sqrt{\eta^2 - 1}$$

$$p_2 = -\eta - \sqrt{\eta^2 - 1}$$

Of course when the damping ratio is less than 1 the poles are complex. The derivation is given in terms of p_1 , p_2 , T_{on} , T_{off} , T , and ρ .

The input to the low pass filter is the switch output which alternates between the two voltages $v_{on} = 1 - \rho$, and $v_{off} = -\rho$. Since the low pass filter has two poles at p_1 and p_2 , the output voltage v_{out} can be expressed for the two time intervals, when the switch is turned on and when it is turned off:

$$v_{out}(t) = A_1 e^{p_1 t} + B_1 e^{p_2 t} + 1 - \rho \quad 0 \leq t \leq T_{on} \quad (C1)$$

and

$$v_{out}^*(t) = A_2 e^{p_1 t} + B_2 e^{p_2 t} - \rho \quad T_{on} \leq t \leq T \quad (C2)$$

At the switching time $t = T_{on}$, v_{out} has to be continuous and also has to have continuous derivative:

$$v_{out}(T_{on}) = v_{out}^*(T_{on}), \text{ and, } \left. \frac{dv_{out}}{dt} \right|_{T_{on}} = \left. \frac{dv_{out}^*}{dt} \right|_{T_{on}} \quad (C3)$$

Evaluating these two equations for A_2 and B_2 (which are, in general, complex constants), we get:

$$\begin{aligned} A_2 &= A_1 + p_2 \cdot e^{-p_1 T_{on}} / (p_2 - p_1) \quad \text{and} \\ B_2 &= B_1 + p_1 \cdot e^{-p_2 T_{on}} / (p_1 - p_2) \end{aligned} \quad (C4)$$

Since v_{out} is also periodic with period T we have to have:

$$v_{out}^*(T) = v_{out}(0), \text{ and, } \left. \frac{dv_{out}^*}{dt} \right|_{=T} = \left. \frac{dv_{out}}{dt} \right|_{=0} \quad (C5)$$

Again, expressing these two equations in terms of v_{out} and v_{out}^* gives us another relationship between A_1 and A_2 or B_1 and B_2 which combined with the equations above give us the values for the four constants A_1 , B_1 , A_2 , and B_2 :

From Equations (C5) we have :

$$A_1 + B_1 + 1 - \rho = A_2 \cdot e^{p_1 T} + B_2 \cdot e^{p_2 T} - \rho \quad (C6)$$

$$\text{and } p_1 \cdot A_1 + p_2 \cdot B_1 = p_1 \cdot A_2 \cdot e^{p_1 T} + p_2 \cdot B_2 \cdot e^{p_2 T} \quad (C7)$$

or solving for A_1 and A_2 we get :

$$A_1 \cdot (p_2 - p_1) + p_2 = A_2 \cdot (p_2 - p_1) \cdot e^{p_1 T} \quad (C8)$$

and for B_1 and B_2 :

$$B_1 \cdot (p_1 - p_2) + p_1 = B_2 \cdot (p_1 - p_2) \cdot e^{p_2 T} \quad (C9)$$

Now , substituting Equ. (C4) into Equ.(C8) - (C9) we finally get :

$$\begin{aligned} A_1 &= \frac{p_2 \cdot (1 - e^{p_1 T_{\text{off}}})}{(p_1 - p_2) \cdot (1 - e^{p_1 T})} \\ A_2 &= \frac{p_2 \cdot (1 - e^{-p_1 T_{\text{on}}})}{(p_1 - p_2) \cdot (1 - e^{p_1 T})} \\ B_1 &= \frac{p_1 \cdot (1 - e^{p_2 T_{\text{off}}})}{(p_2 - p_1) \cdot (1 - e^{p_2 T})} \\ B_2 &= \frac{p_1 \cdot (1 - e^{-p_2 T_{\text{on}}})}{(p_2 - p_1) \cdot (1 - e^{p_2 T})} \end{aligned} \quad (C10)$$

Equations (C10) express all four constants A_1 , A_2 , B_1 , and B_2 in terms of the converter parameters. In order to find the maximum and the minimum of the function $v_{out}(t)$, we have to evaluate its derivative, which has to be zero at the extrema. Assuming that one occurs at $t = t_1$ and the other at $t = t_2$, and also that one occurs during the interval $0 \leq t \leq T_{on}$, and the other in the interval $T_{on} \leq t \leq T$, we have :

$$\left. \frac{dv_{out}}{dt} \right|_{t=t_1} = \left. \frac{dv_{out}^*}{dt} \right|_{t=t_2} = 0 \quad (C11)$$

or evaluating t_1 and t_2 we get :

$$t_1 = \frac{\ln(-p_2 \cdot B_1 / p_1 \cdot A_1)}{p_1 - p_2}, \text{ and} \quad (C12)$$

$$t_2 = \frac{\ln(-p_2 \cdot B_2 / p_1 \cdot A_2)}{p_1 - p_2},$$

and substituting t_1 and t_2 into equations (C1) and (C2) we get :

$$v_{ripple} = \left| A_1 e^{p_1 t_1} + B_1 e^{p_2 t_1} + 1 - A_2 e^{p_1 t_2} - B_2 e^{p_2 t_2} \right| \quad (C13)$$

and the percentage output ripple we get by :

$$\text{Percentage output ripple} = 100 \cdot v_{ripple} / \rho \quad (C14)$$

which gives us our desired result.